METEOR Berichte

Climate Archives in Coastal Waters of Southern Africa

Cruise No. M123

February 03 – February 27, 2016
Walvis Bay (Namibia) – Cape Town (Rep. of South Africa)

M. Zabel
and cruise participants

Editorial Assistance:

DFG-Senatskommission für Ozeanographie
MARUM – Zentrum für Marine Umweltwissenschaften der Universität Bremen

2016

The METEOR-Berichte are published at irregular intervals. They are working papers for people who are occupied with the respective expedition and are intended as reports for the funding institutions. The opinions expressed in the METEOR-Berichte are only those of the authors.

The METEOR expeditions are funded by the *Deutsche Forschungsgemeinschaft (DFG)* and the *Bundesministerium für Bildung und Forschung (BMBF)*.

Editor:
DFG-Senatskommission für Ozeanographie
c/o MARUM – Zentrum für Marine Umweltwissenschaften
Universität Bremen
Leobener Strasse
28359 Bremen

Author:
Dr. Matthias Zabel
MARUM, Universität Bremen
Leobener Str.
D-28359 Bremen

Telefon: +49 421 218 65103
Telefax: +49 421 218 9865103
E-Mail: mzabel@uni-bremen.de

Citation: M. Zabel and cruise participants (2016) Climate Archives in Coastal Waters of Southern Africa – Cruise No. M123 – February 3 – February 27, 2016 – Walvis Bay (Namibia) – Cape Town (Rep. of South Africa). METEOR-Berichte, M123, 50 pp., DFG-Senatskommission für Ozeanographie, DOI:XXX

ISSN 2195-8475

Table of Contents

		Page
1	Summary / Kurzfassung	1
2	Participants	2
3	Research Program and Narrative of the Cruise	3
4	Preliminary Results	5
	4.1 Acoustic Surveys	5
	4.2 Sediment sampling	10
	4.3 Physical Properties	11
	4.4 Mineralogy	21
	4.5 Microfossils	25
	4.6 Plankton Sampling	38
	4.7 Sampling of Surface Water Suspended Material	40
	4.8 Water Sampling	41
5	Ship's Meteorological Station	42
6	Station List	44
7	Data and Sample Storage and Availability	45
8	Acknowledgments	45
9	References	46

1 Summary / Kurzfassung

This research cruise M123 was directly connected to the collaborative research project RAiN (*Regional Archives for Integrated iNvestigations*) which is funded by the Ministry of Education and Research (BMBF) in the framework of the SPACES program (*Science Partnerships for the Assessment of Complex Earth System Processes*). The overreaching goal of this project is to expand the current state of knowledge on the drivers and dynamics of South African Late Quaternary climate change by directly comparing marine and terrestrial proxy-records. Whereas sufficient sample material for these analyses was retrieved from the western South African coast during former expeditions, suitable marine sediment cores with high resolution deposits were not available from the south and east coast of southern Africa until now. This was, in part, due to patchy records affected by the regional style of dominant sedimentation regimes along these shores, which are influenced primarily by the strong south-westward flowing Agulhas contour current which causes erosion and sediment redistribution processes rather than accumulation and preservation. As we suspected and now proved true, based on detailed information on surface sediment characteristics and recent geomorphological studies of the shelf and continental slope areas, both provided by the South African co-proponents and partners, we could find the small-scale Holocene sediment bodies with sufficient thickness and were able to retrieve long sediment cores in front of all major rivers along the coast of southern Africa up to the Limpopo River. Depending on sediment grain size and texture, sea floor samples were taken with gravity corer, vibrocorer, box corer and multicorer. Surface samples and sediment cores could be retrieved at 25 sites from water depth between 32 m and 3.059 m, with a total recovery length of more than 107 m. For the purpose of identifying the best locations for coring, the ship's acoustic systems were used along more than 900 nm of profile lines. In addition to the sediment work, at six sites planktonic foraminifera could be sampled using a multinet. Beside the scientific goals of this expedition, a strong focus was placed on the training of young scientists and advanced students from Germany and South Africa.

Die Expedition M123 stand im unmittelbaren Zusammenhang mit dem deutsch-südafrikanischen Forschungsverbundvorhaben RAiN (*Regional Archives for Integrated iNvestigations*), welches durch das Bundesministerium für Bildung und Forschung (BMBF) finanziert wird und Teil des SPACES-Programms (*Science Partnerships for the Assessment of Complex Earth System Processes*) ist. Das übergeordnete, wissenschaftliche Ziel in RAiN ist die Erweiterung des aktuellen Kenntnisstandes zur Steuerung und Dynamik der spätquartären Klimavariabilität im südlichen Afrika. Der Schlüssel hierzu wird unter anderem in Vergleichen zwischen terrestrischen und marinen Sedimentarchiven gesehen. Während es aufgrund vorheriger Expeditionen genügend Probenmaterial für entsprechende Untersuchungen von der Westküste Südafrikas gibt, konnten von der Süd- und Ostküste keine Sedimentkerne mit hinreichend zeitlich hochauflösenden Ablagerungen gewonnen werden. Dies ist den regionalen Sedimentationsbedingungen zuzuschreiben, die insbesondere küstennah durch den süd-westlich fließenden Agulhas-Strom bestimmt werden, wodurch stark erosive Umlagerungsprozesse hervorgerufen werden. Wie von uns erwartet und durch die Ergebnisse dieser Expedition bestätigt, lassen sich auf Basis neuerer geomorphologischer Studien und vorhandener Informationen zu Verteilungsmustern von Oberflächensedimenten dennoch kleinräumige holozäne Sedimentkörper mit hinreichender Mächtigkeit vor allen Flussmündungen des

südlichen Afrika finden. Der Erfolg der Ausfahrt M123 wurde maßgeblich durch die enge Zusammenarbeit mit den südafrikanischen Partnern bzw. deren Zurverfügungstellung von Detailinformationen ermöglicht. Je nach Korngrößenspektrum der Ablagerungen wurden zur Probennahme Schwerelot, Vibrolot, Großkastengreifer und/oder Multicorer eingesetzt. Insgesamt konnten an 25 Lokationen Oberflächensedimente aus Wassertiefen von 32–3.059 m gewonnen werden. Die Gesamtlänge der mit Loten gewonnen Kerne beträgt 107 m. Um die bestmöglichen Lokationen zur Probennahme zu finden wurden die akustischen Systeme des FS Meteor auf Profilfahrten von über 900 nm Länge eingesetzt. Zur Beprobung planktischer Foraminiferen in der Wassersäule erfolgten ferner an sechs Stationen erfolgreiche Einsätze eines Multischließnetzes. Neben der Verfolgung wissenschaftlicher Ziele lag ein besonderer Fokus dieser Expedition auf der praktischen Ausbildung junger Wissenschaftler und fortgeschrittener Studenten aus Deutschland und Südafrika.

2 Participants

Tab. 2.1 List of scientific party

Name	*Discipline*	*Institution*
Zabel, Matthias, PD Dr.	Sediment Geochemistry / Chief Scientist (CS)	MARUM
Amberg, Sebastian	Student	MARUM
Andò, Sergio, Prof. Dr.	Sedimentology	UNIMIB
Bergh, Eugene, PhD-stud.	Student	UCT-Geo
Cawthra, Hayley, Dr.	Marine Geology	CG
Du Plesis, Nadia, PhD-stud.	Student	UCT-EGS
Eichenauer, Christian, Ing.	Documentation	*(Freelancer)*
Frederichs, Thomas, Dr.	Geophysics	GeoB
Frenzel, Peter, PD Dr.	Micropaleontology	FSUJ
Gander, Lukas	Student	FSUJ
Gilson, Dirk, Journalist	Documentation	*(Freelancer)*
Gomes, Megan	Student	UW
Green, Andrew, Prof. Dr.	Geomorphology; Co-CS	UKZN-Geo
Hahn, Annette, Dr.	Sediment Geochemistry	MARUM
Higgs, Caldin	Student	UW
Hinkeldey, Alexander	Student c	GeoB
Hoffmann, Daniel	Student	GeoB
Humphries, Marc, Dr.	Geochemistry	UW
Kossack, Michael	Student	MARUM
Maboya, Matjie Lilian	Student	UCT-EGS
Khumalo, Vamamusa	Student	UCT-Geo
Pillay, Talicia	Student	UKZN-Geo
Pretorius, Lauren	Student	UKZN-Geo
Rohleder, Christian, Met.	Meteorology	DWD
Siccha, Michael, Dr.	Micropaleontology	MARUM
Schade, Tobias, Tech.	Technology	MARUM
Schefuß, Enno, Dr.	Organic Geochemistry	MARUM
Stelzner, Martin, Tech.	Meteorology	DWD

Strachan, Kate, Dr.	Micropaleontology	UKZN-ES
Wiles, Errol, Dr.	Geomorphology	UKZN-Geo

Participating Institutions

CG	Council for Geosci., Geophys. Competency – Marine Geosci. Unit, 3 Oos Street, 7535 Bellville, South Africa	www.geoscience.org.za
DWD	Deutscher Wetterdienst, Geschäftsfeld Seeschifffahrt, Bernhard-Nocht-Str. 76, D 20359 Hamburg, Germany	www.dwd.de
GeoB	Dept. of Geosciences, Bremen University Klagenfurter Str., D 28359 Bremen, Germany	www.geo.uni-bremen.de
FSUJ	Friedrich-Schiller-Univ. Jena, Institute of Geosciences, Burgweg 11, 07749 Jena, Germany	www.igw-ahg.uni-jena.de
MARUM	Centre for Marine Environmental Sciences Leobener Str., D 28359 Bremen, Germany	www.marum.de
UCT-EGS	University of Cape Town, Dept. of Environmental Geographical Sci., 7701 Rondebosch / South Africa	www.egs.uct.ac.za
UCT-Geo	University of Cape Town, Dept. of Geological Sci., 7701 Rondebosch / South Africa	www.geology.uct.ac.za
UKZN-ES	University of KwaZulu-Natal, Environ. Sci. / Phys. Geography, 4000 Westville / South Africa	www.ukzn.ac.za
UKZN-Geo	University of KwaZulu-Natal, Geology – Mar. Geol. Res. Unit, 4000 Westville / South Africa	www.ukzn.ac.za
UNIMIB	Univ. of Milano Bicocca, Dept. of Earth and Environ. Sci., Piazza della Scienza 4, 20126, Milano, Italy	www.geo.unimib.it
UW	Univ. of the Witwatersrand - Faculty of Science – School of Chemistry, Private Bag 3, 2050 PO WITS / South Africa	www.wits.ac.za/chemistry

Fig. 2.1 Scientific party on M123

3 Research Program and Narrative of the Cruise

(M. Zabel)

Our research program concentrated on three main working areas along the south- and east-coasts of southern Africa. On the south coast off Mossel Bay and on the east coast south of Durban, we continued a first sampling campaign, which started successfully in December 2013 on R/V

METEOR expedition M102. The third area was the outer Maputo Bay, where we expected to find deposits consisting of sediments from the Limpopo River catchment. From two former expeditions (M63-1 and M75-3) seismic information exist, which have been published in the meantime and now could be used to better understand the regional sediment distribution pathways and to identify areas with high accumulation rates during the Late Quaternary. Due to the lack of detailed information from the shelf areas, on both previous expeditions shallow water areas were not searched for fine-grained deposits, which are a prerequisite for most investigations when the target is to identify and decipher climate signals in terrigenous sediments. Instead, both cruises had focused on the continental slope.

Fig. 3.1 Cruise trajectory and sampling sites.

The expedition started in the morning of February 3 from the harbor of Walvis Bay (Namibia). Due to the very long transits (from Walvis Bay (Namibia) to the other side of the continent (Mozambique) and back to Cape Town) and taking the current pattern into account, we decided to start our pre-site surveys in Mozambican waters off the Limpopo River Mouth. On the 10-day-transit one gravity core in the southern Cape Basin and a first set of surface sediments at four sites on the narrow east coast shelf were taken. We had to learn that the patches of more muddy sediments are very local and very restricted, that it takes some effort to identify them with the PARASOUND system and that it is even more difficult to sample them. Although the grain sizes spectrum of the minerals showed a great variety, heavy mineral assemblages could already be assigned to different source areas. On February 12 we arrived at the first location in working area 1 (GeoB20607). During the next nearly five days nine successful gravity corer deployments followed at 11 sites. On Tuesday, February 16, we left working area 1 and started to return. With the strong Agulhas stream the vessel made rapid progress. At about 29,4°S,

31,5°E we found a several meter thick package of muddy sediments north of the Tugela River mouth in about 32m water depth. At this location we could retrieve three up to 8,26 m long sediment cores, a very unusual procedure at a very unique site. According to the previous plan the work was carried out successively in both other working areas. After 25 days with mostly very favorable weather conditions the expeditions ended in the early morning of February 27 in the harbor of Cape Town.

4 Preliminary Results

4.1 Acoustic Surveys *(Parasound and Multibeam)*

(A. Green, H. Cawthra, A. Hinkeldey, M. Humphries, V. Khumalo, L. Pretorius, K. Strachan & E. Wiles)

Continuous PARASOUND and multibeam bathymetric profiling was undertaken since entering South African waters on the 5th February 2016. The primary aim of the hydroacoustic surveying was to identify suitable fine-grained sediment deposits on the shelf and upper slope offshore the main fluvial entry points to the south and west coasts of South Africa and southern Mozambique.

In addition to the newly collected data, existing local datasets were used as reference (e.g. the past and ongoing work of South African marine geologists in RAiN), as well as a series of older published marine geological maps of the South African shelf (Birch et al., 1986). These maps allowed the sites to be constrained according to surficial textures and sediment characteristics, although the compilations were not based on cores, but surficial samples which were obtained from 1967 – 1981. These proved particularly beneficial in identifying the loci of muddy sediments on the shelf.

Working area 1, offshore the Limpopo River/Maputo Bay is characterised by a broad depositional cone. Figures 4.1 to 4.3 show the location of the most prominent cores acquired in the area. All depth scales are in milliseconds two way travel time. The shelf edge and upper slope comprise sigmoid prograding, moderate to high amplitude reflectors (Fig. 4.1 and 4.2). At least two sets of sigmoid packages are evident, the lowermost truncated by a strongly erosional surface onto which the younger package of sigmoid reflectors onlap (Fig. 4.2). This erosional surface extends beneath the shelf and forms a series of small scale incised valleys that become prominent from depths of 70 m (90 ms) to landwards. Overlying this surface are small incised valley fill sequences, in addition to the second sigmoid prograding unit in the more distal part of the shelf-upper slope. First interpretations of the data suggest a lowstand shelf valley system that fed material to a lowstand shelf edge delta. This unit is similarly truncated by a second, high amplitude reflector that extends onto the outer to mid-shelf. This reflector is less rugged and more planar than the lower erosional unconformity. Overlying this surface are a series of acoustically transparent units that onlap a series of rugged pinnacles and ridges (Fig. 4.2 and 4.3). These ridges overlie the incised valleys of the lowermost erosional reflector. Early interpretations consider these post-glacial features that overlie the last glacial maximum subaerial unconformity. Green et al. (2014) interpret these from the adjoining shelf in South Africa as drowned barrier shoreline systems. The onlapping transparent facies are correlated to the post-glacial early shoreface that developed near contemporaneously with the barriers. The unconformity separating the two marks the wave ravinement surface that formed as the shoreface translated over the old barrier-shelf profile. The lee of the barriers comprises either high

amplitude laminated to acoustically opaque reflectors (Fig. 4.2) or by acoustically transparent internally featureless units (Fig. 4.3). GeoB20610 revealed that the former comprises muddy deposits, thought to be contemporaneously forming back-barrier lagoonal sequences. Preliminary microfossil analyses however indicate the mud is devoid of any brackish species and is likely a fluvial deposit housed in the available accommodation behind the barrier form. The latter comprises sandy shoreface material as evidenced from boxcore GeoB20612.

The mid to inner shelf appears to be controlled by the deposition of material from the main river sources that is reordered by waves and longshore currents into a shallow, wave-dominated delta. Variably dipping reflector arrangements (Fig. 4.2) that merge landwards into an onshore prograding beachridge field attest to this.

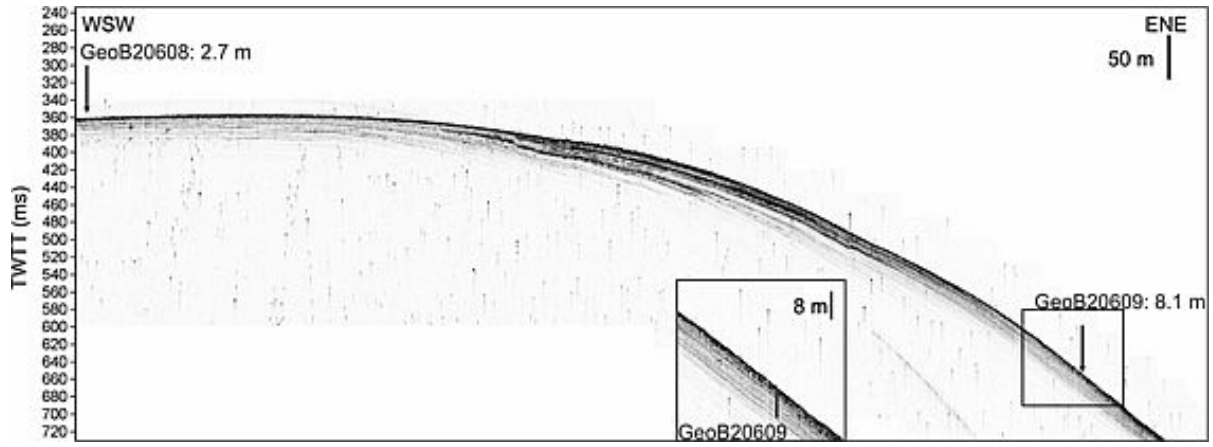

Fig. 4.1 PARASOUND profile depicting locations of GeoB20608 and GeoB20609. Both were acquired on a slope terrace with thick (>20 ms) laminated sediments.

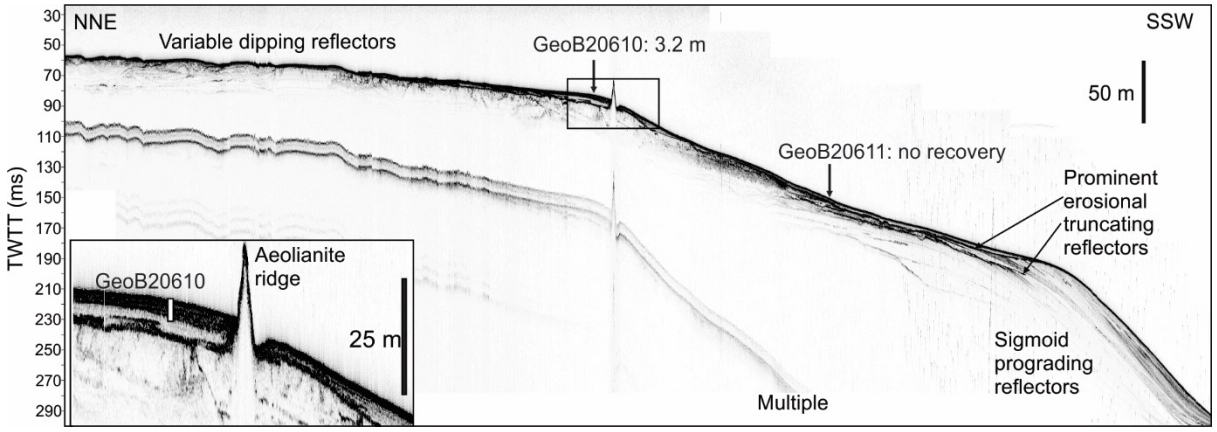

Fig 4.2 Location of GeoB20610 in the landward lee of an aeolianite.

Working area 2 encompasses the shelf offshore the Tugela and Mzimvubu River's. For brevity's sake, the Tugela alone is discussed here. The stratigraphy comprises a shallow bedrock basement (Cretaceous siltstones), which crops out in places, overlain by thin (<15 ms) sediment cover in the mid-outer shelf (Fig. 4.4). Like the Limpopo area, this is interrupted by pinnacles and ridges against which the unconsolidated material onlaps. These features are similarly interpreted as aeolianite barrier ridges with an onlapping postglacial shoreface respectively. At a depth of ca. 40m (50ms), the sandy shoreface is overlain by a thick blanket of mud. The exact thickness is unclear due to gas curtaining (Fig. 4.4), however at least 8,3 m of clay-rich material was

retrieved by GeoB20619-3. This mud forms the prodelta of the wave-dominated Tugela subaqueous delta.

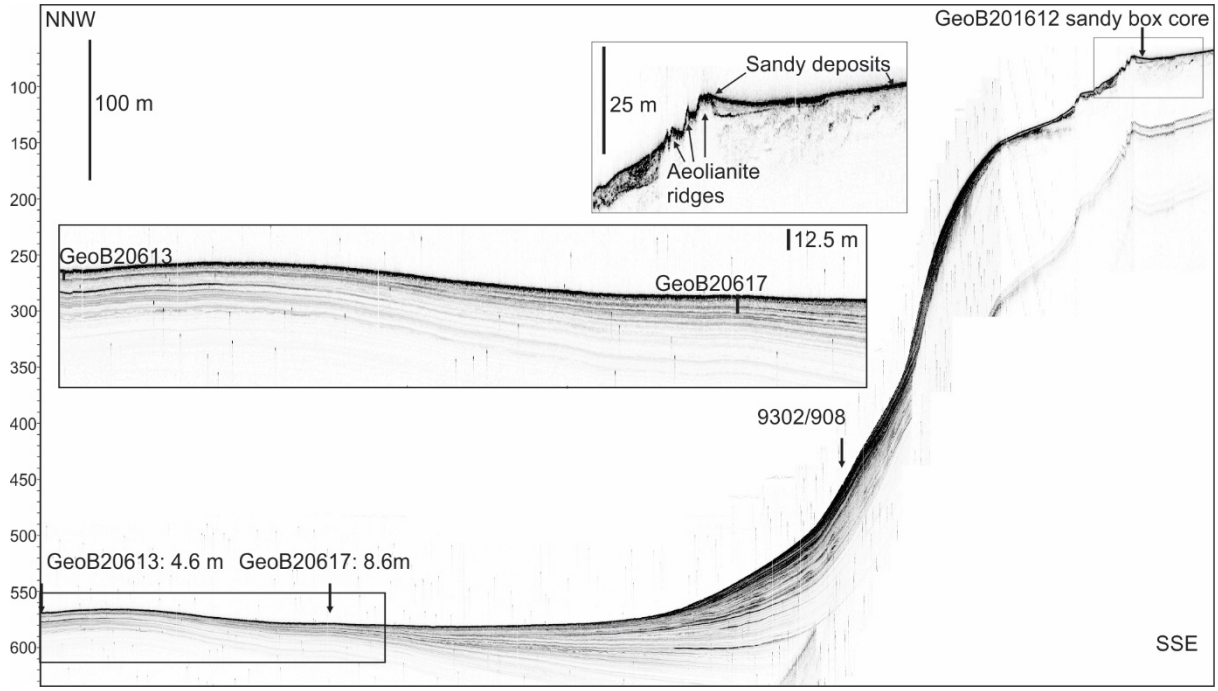

Fig. 4.3 Location of GeoB20613, GeoB20617 and boxcore GeoB20612. Note the sandy lee behind the aeolianite.

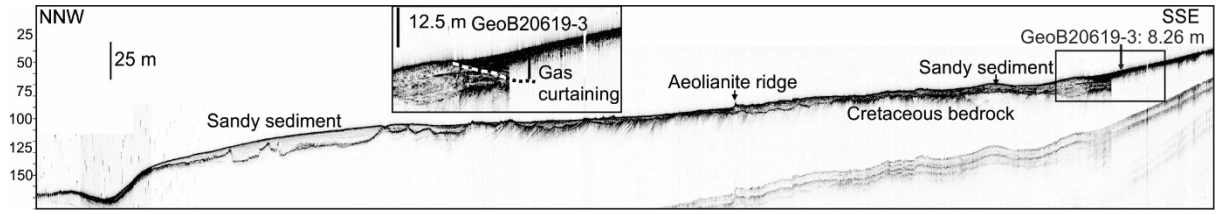

Fig. 4.4 PARASOUND profile of the Tugela Delta. GeoB20619-3 retrieved 8,26 m of muddy sediment from a gassy layer in the acoustic profile.

One box core (GeoB20603-1) and one gravity core (GeoB20623-1) were taken off the Mzimvubu River on the continental shelf of Port St Johns. A major canyon extends offshore, towards the east, and is incised to at least 500 m below the surrounding seafloor (Fig. 4.5). Accumulations of sediments were identified on the multibeam echosounder, within the structural features and morphology conducive to entrapment within the canyon. The surface texture and acoustic characteristics of these sediments suggested that they may represent terrestrial deposits and an appropriate site was identified.

Working area 3, the South Coast of South Africa, was surveyed for the purposes of reconnaissance using PARASOUND and multibeam bathymetry, and two vibrocores were obtained from this region. GeoB20628-1 was obtained east of the Breede River mouth. The maps of Birch et al. (1986) showed surficial muds which have been postulated to constitute a South Coast mud belt. In this region, sand delivered by rivers is transported east by longshore drift, while suspended mud is likely distributed further offshore and transported west by bottom currents to form the South Coast mud belt (Cawthra, 2014). According to this conceptual model, a -45 m nick point on the South Coast shelf provides accommodation space for the inshore

sediment wedge to be preserved and gentle slope of the mid shelf is a likely area of accretion for the muddy deposits, protected from open ocean swells compared to the flat Agulhas Bank. The vibrocore penetrated through this mud deposit and the basal Cretaceous siltstones, revealing a ravinement surface at the contact which is likely remnant of at least the Holocene Transgression. Initial microfossil analyses have confirmed that this mud unit is populated with marine species.

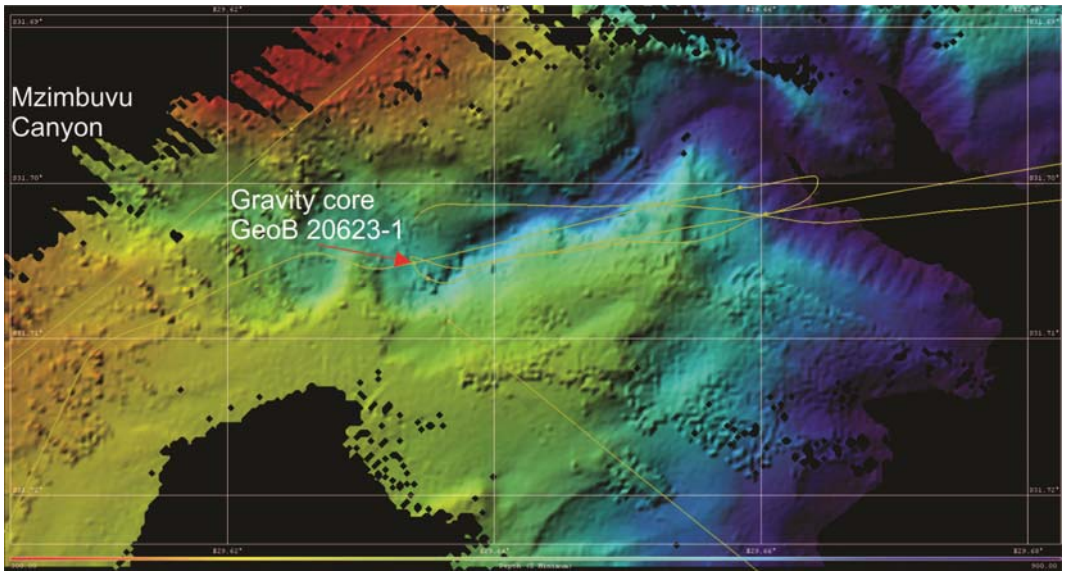

Fig. 4.5 Location and context of core GeoB20603-1, with multibeam bathymetry as the base. GeoB20623-1 was obtained from the same canyon, at a water depth of 1000 m.

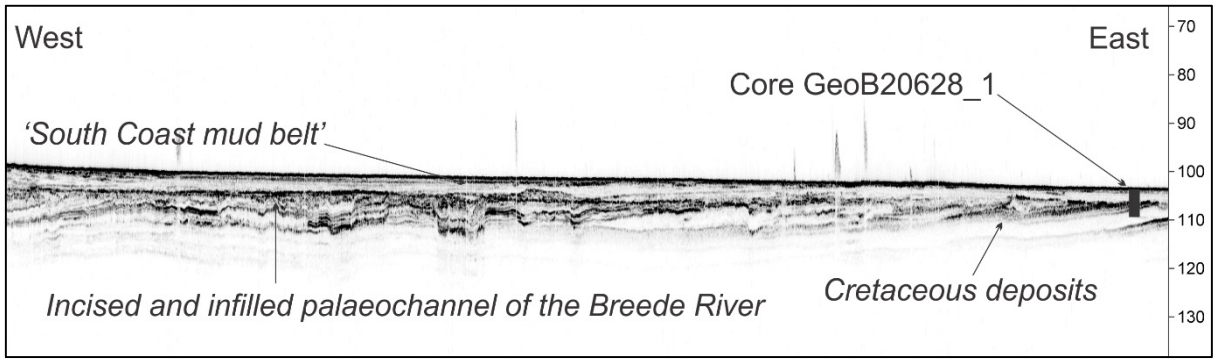

Fig. 4.6 PARASOUND profile showing the core site of GeoB20628-1 east of the Breede River. The y-axis indicating the vertical scale is indicated as two-way travel time in milliseconds.

Vibrocore GeoB20629-1 was obtained from a depth of 54 m offshore of the Wilderness Embayment. Here, during sea-level regressions, both the incision of fluvial channels and the deposition of back-barrier systems occurred across the continental shelf (Cawthra et al., 2014). During late low stand/early transgression periods, landward shoreface migration occurred and pre-existing channel incisions were infilled and pre-existing barriers were truncated. Rapid transgression, however, allowed the preservation of some back-barrier deposits, possibly aided by protection from antecedent topography. As sea level neared the present-day elevation, erosion of the mid-shelf sediments resulted in the development of a Holocene sediment wedge. At this site, however, the Holocene sediment wedge does not form a thick cover sequence blanketing these well-preserved terrestrial sediments.

Two Kongsberg multibeam bathymetry systems were used during the M123 cruise. The EM122, a deep water system was used alongside the EM710 shallow/mid water system. Each system was used to acquire data within respective operational water depths which allowed the best possible resolution data to be collected along transects and during transit between working areas.

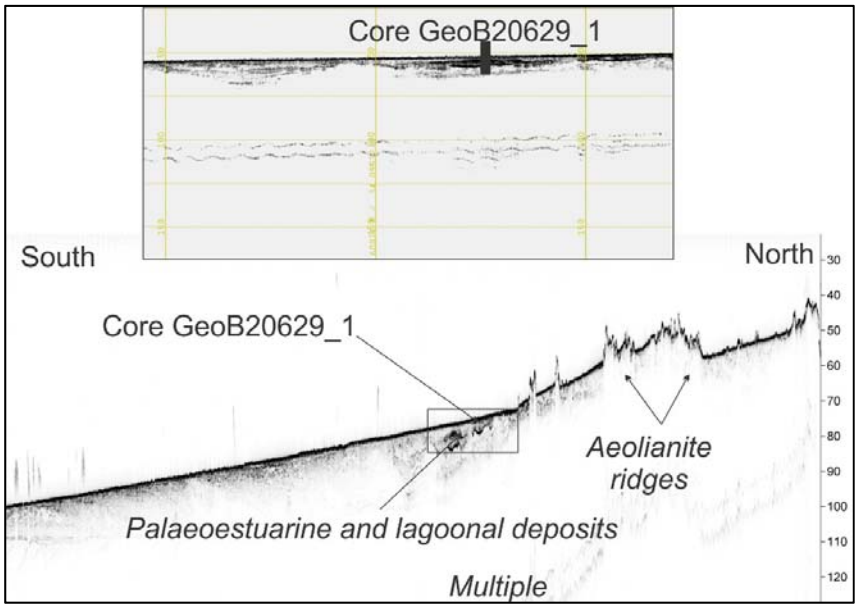

Fig. 4.7

PARASOUND profile showing the core site of GeoB20629-1 south of the Wilderness Embayment. The y-axis indicating the vertical scale is indicated as two-way travel time in milliseconds.

The multibeam data were used in conjunction with PARASOUND data to confirm seafloor types observed on the PARASOUND data. The combined data sources were essential in identifying the site of the Mzimvubu River core, GeoB20623-1, located in the upper reaches of the Mzimvubu Canyon (Fig. 4.5).

During calm conditions the widest beam angle (70°) was used to collect the widest useful swath of data; the beam angle reduced as sea conditions deteriorated. Sound velocity profiles were acquired using SVP-XBTs which were deployed during deep stations. Regular artifacts observed in the EM710 data were attributed to acoustic interference between the EM710 and PARASOUND systems whereby the PARASOUND pulse would attenuate the multibeam swath in regular, track oblique, stripes (Fig. 10). This effect was most noticeable in shallow areas when using a template to maximize PARASOUND data quality above -100 m.

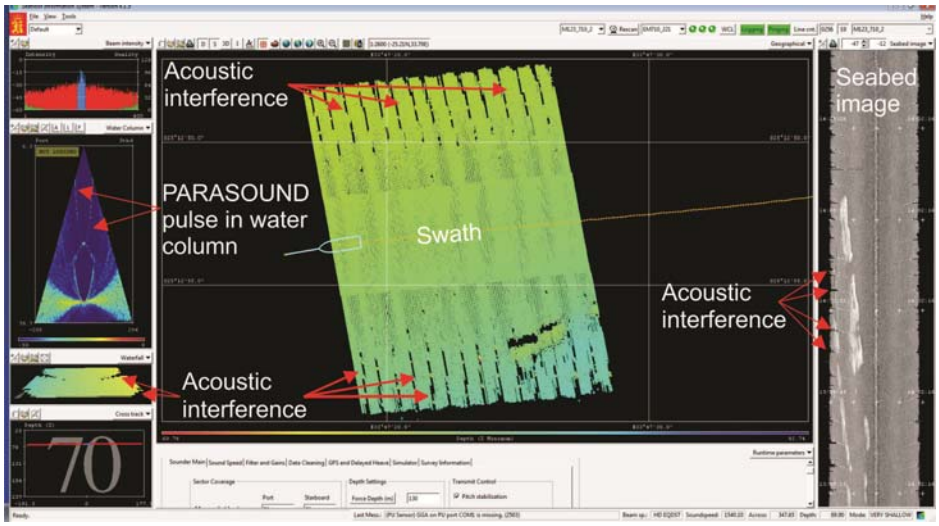

Fig. 4.8

Negative effect of PARASOUND pulse on EM710 multibeam data is shallow waters

4.2 Sediment Sampling

(E. Schefuß, S. Amberg, N. Du Plesis, A. Hahn, M. Kossack, T.Pillay)

During the M123 cruise four different devices were used to sample ocean bottom sediments, i.e. the box corer (BC), the multi-corer (MC), the gravity corer (GC) and the vibro corer (VC). While BC and GC were used at the majority of stations, the MC and VC were only used at selected stations at which fine-grained or coarse-grained material, respectively, could be expected.

Sediment sampling with box corer (BC)

At sites with unknown surface sediment cover, the BC was deployed first to achieve an impression of the bottom sediment layer. From all box cores, the surface sediment layer (0-1 cm) was sampled for investigation of the benthic foraminiferal fauna and heavy mineral content. In cases where coarse-grained surface sediments were recovered, no additional samples were taken. In cases where fine-grained surface sediments were recovered, 2 petri-dish samples of the sediment surface (0-1 cm) were taken, sealed and stored at room temperature. Additionally, a core liner was pressed into the sediment to retrieve an archive of the sampled material. This liner was cut, sealed with end-caps and stored at room temperature. The remainder of the intact surface (0-1 cm) of the BC was scraped off and put into a plastic bag which was stored at room temperature afterwards.

Sediment surface sampling with multicorer

In cases of fine-grained surface sediments, the MC was deployed for recovery of undisturbed sediment surfaces. The MC was equipped with 8 tubes of 10 cm and 4 smaller tubes of 5 cm in diameter. The MC was used at 3 stations in the Limpopo area. During all MC deployments sampling was successful resulting in all filled cores. The surface (0-1 cm) of 2 large cores was transferred into petri-dishes, which were sealed and stored at room temperature. Two other large cores were used for surface sediment sampling (0-1 cm) for heavy minerals and benthic foraminifera. Two other large tubes (equipped with cut VC-liners) were stored at room temperature as archives. Due to the lack of appropriate sampling material, the remainder of the recovered material was discarded.

Sediment sampling with gravity corer and vibrocorer

During the M123 cruise 16 sediment cores were recovered using the gravity corer SL-12, and SL-6. The vibrocorer was used at 3 sites for which sandy sediments were expected. Once a core was retrieved on the deck, the core liners were cut into 1 m segments, closed with caps at both ends and labelled according to the scheme applied in MARUM and the Geosciences Department, University Bremen. All cores were cut along-core in two half pieces: one archive and one work-half. The sediment sections were described according to IODP rules. The archive halves were then scanned immediately after opening using a smartcube© camera image scanner taking digital photos. Camera scanner readings of the ratio 700 nm/400 nm (red/blue ratio) and L* of the core sediments were derived from these scans. From the work-half one series of samples (ca. 5 ccm) was taken at irregular intervals. These samples were taken for discrete XRF measurements at MARUM. Additional samples (ca. 1 per section) were taken for the analysis of heavy mineral associations and benthic foraminiferal ecology.

The preliminary lithologic summary of the sediments retrieved with the gravity corer is based on visual description and scanner data.

4.3 Physical Properties

(T. Frederichs, M. Gomes, C. Higgs, A. Hinkeldey, M. Khumalo)

4.3.1 Methods

The sediment series recovered during R/V METEOR Cruise M123 by gravity and vibro coring were subject to routine laboratory geophysical studies. Shipboard measurements on the segmented cores were made using a Geotek Multi-Sensor Core Logger (MSCL) and a smartcube® Camera Image Scanner smartCIS. The MSCL measurements routinely comprise two basic physical parameters:

- electrical resistivity R_s (as a measure of porosity and density),
- magnetic volume susceptibility κ

Digital imaging utilizing by the smartcube® Camera Image Scanner smartCIS provided high resolution down-core images with additional light and color reflectance parameters.

These properties are closely related to the lithology and grain size of the sediments. Electrical resistivity and magnetic volume susceptibility yield medium-resolution core logs available prior to all other detailed investigations. The characteristic sensor response width for these parameters is approximately 5-8 cm and all the cores were measured at 1 cm resolution. Magnetic susceptibility and electrical resistivity were measured on closed cores, after letting them warm for a few hours at room temperature. The archive half of each sampled core was optically scanned at a resolution of 0.005 cm to obtain digital photographs and light reflectance curves.

Magnetic Volume Susceptibility

Magnetic volume susceptibility κ is defined by the equations

$$B = \mu_0 \cdot \mu_r \cdot H = \mu_0 \cdot (1 + \kappa) \cdot H = \mu_0 \cdot H + \mu_0 \cdot \kappa \cdot H = B_0 + M$$

with magnetic induction B, absolute and relative permeabilities μ_0 and μ_r, magnetizing field H, magnetic volume susceptibility κ and volume magnetization M. It can be inferred from the third term, κ is a dimensionless physical quantity. It represents the amount to which a material is magnetized by an external magnetic field.

For marine sediments the magnetic susceptibility may vary, between an absolute minimum value of around $-15 \cdot 10^{-6}$ SI units (diamagnetic value of pure carbonate or silicate) to a maximum of some $10.000 \cdot 10^{-6}$ SI for basaltic debris rich in (titano-) magnetite. In most cases κ is primarily determined by the ferrimagnetic mineral content, while paramagnetic matrix components such as clays are of minor importance. High magnetic susceptibilities indicate high terrigenous or low carbonate deposition. Low values of magnetic susceptibility can also result from post-depositional reduction of oxic iron minerals. In absence of pervasive diagenesis, magnetic susceptibility can serve for a correlation of sedimentary sequences deposited under similar conditions. For long-core measurements a commercial Bartington MS2 susceptibility meter with a 140 mm loop sensor is mounted on the Geotek MSCL. The Bartington MS2 has an operating frequency of 0.565 kHz and effective resolution of $2 \cdot 10^{-6}$ SI. Due to its size, the sensor integrates

the response signal over a core interval of about 8 cm. Consequently, sharp susceptibility changes in the sediment column appear smoothed in the κ log.

Electrical Resistivity, Porosity, and Density

The electrical sediment resistivity R_s was determined using an external inductive sensor. A platinum resistance thermometer (PRT) was used to measure the temperature of a reference core section. For sensor calibration, a series of saline solutions were measured daily. This calibration is applied to the measured voltage data during post-processing.

The porosity ϕ was calculated according to the empirical Archie's equation,

$$R_s/R_w = k \cdot \phi^{-m}$$

which approximates the ratio of sediment resistivity R_s to pore water resistivity R_w by a power function of porosity ϕ. Following a recommendation by Boyce (1968) for sea water saturated clay-rich sediments, values of k=1.30 and m=1.45 were used. Density estimates were calculated assuming a mean bulk density of 2670 kg/m^3. For inductive porosity and susceptibility proxies, we joined the core section data to an entire core log due to a method-immanent non-linear signal decay toward the section caps. Corrections using an adapted core end correction curve were applied, but some conspicuous peaks and discordances persist at some section boundaries and should not be over-interpreted.

Light Reflectance

The smartcube® Camera Image Scanner smartCIS is a special device to make scans of slabbed and unrolled cores, to create digital archive copies of split core surfaces. The included software package smartSCAN contains a special interface to communicate with the smartDIS-database.

The digital imaging module of the smartCIS consists of a line-scan camera with triple color sensor (3 x 4080 Pixel) and lenses with focal lengths of 50 and 75 mm. The camera module measures the reflected light from two fluorescent tubes illuminating the core from a height of ~5 cm. Archive halves of the core sections were prepared to give a smooth surface. Cores were usually scanned at a resolution setting of 500 dpi (20 pixel per mm core depth), Depth-of-field mode set to true/medium and a lens aperture of f8 with auto correction set to off.

The settings used for each core are saved to the respective data files. A white light calibration was conducted at the beginning of each core taken from a specific site, or when the aperture was changed. This involves measuring the response of the camera to a white tile of known reflectance (white calibration).

As part of the post-processing, end-caps were removed from the line scan image. Artifacts were then identified on the R/B ratio and L graphs and removed. Among other parameters, for each processed core, the smartCIS software construct depth series for the red, green and blue color channels, L value (in percent, as measure of total reflectance) and the ratio of the red to blue channels. L was calculated by the following equations:

$R' = R/255,\ G' = G/255,\ B' = B/255$

$L'_{max} = \max(R', G', B'),\ L'_{min} = \min(R', G', B')$

$L' = \mathrm{INT}\ (L'_{max} + L'_{min}) / 2)$

$L^* = L' \cdot 100\%$

For visualization purposes, two digital core scans of each core were prepared and plotted in all core logs. The first image shown to the left of each figure represents a non-modified 'realistic' photograph of the sediment surface. A second image shown adjacent to the right was enhanced by modifying the contrast to a value of 75 on a scale ranging between -127 and +127 in order to emphasize core optical features (cf. Figs. 4.13 – 4.16).

4.3.2 Shipboard Results

The means and trends of the porosity and susceptibility measurements, as well as core lengths and water depths, are compiled in Fig. 4.9. Dots indicate the mean values of porosity, derived density and magnetic susceptibility. Vertical error bars denote the standard deviations. Each diagram is divided into groups of spatially adjacent cores. Color statistics are not included as absolute reflectance numbers are controlled by multiple factors and therefore not easy to compare.

Average porosities calculated for gravity cores ranged from about ca. 40% to 56%. Porosity values in their lower range appear exceptionally dense for unconsolidated marine sediments. Most porosity values are slightly above 45%. The lowest value (about 40%) was determined for core GeoB20624-1 which came from deeper water depths, in extension of the Mzimvubu River mouth. This is in clear contrast to the porosity of 56% measured for the other deep-water core GeoB20620-4 from the Natal Valley which represented the highest mean porosity of all the cores. In summary, porosity does not demonstrate any clear dependence on water depth. Corresponding to low mean porosities, densities are relatively high ranging from 1744 kg/m³ (GeoB20620-4, water depth 3059 m) to 2012 kg/m³ (GeoB20624-1, water depth 2644 m), again indicating no clear general trend.

Porosity and density data for vibrocore GeoB20622-2 are not shown in Fig. 4.9, since these values seem to be biased to non-realistic values, due to pore water loss during coring. Voids that are not completely filled with pore water result in significantly reduced electrical resistivity and thus decreased porosities and increased densities.

The volume magnetic susceptibility means for cores from the east and south coast are in the ca. 42 to $852 \cdot 10^{-6}$ SI range. Core GeoB20609-2 from the deeper part of the Limpopo area shows the highest mean susceptibility ($852 \cdot 10^{-6}$ SI). This is more than three times the value of the adjacent core GeoB20613-2 showing a mean susceptibility of $269 \cdot 10^{-6}$ SI, which was recovered from similar water depth. Absolute values of magnetic susceptibility of several $100 \cdot 10^{-6}$ SI (40-$2600 \cdot 10^{-6}$ SI) are not as low as in areas dominated by more biogenic material as can been seen from core GeoB20604-1 (mean $7 \cdot 10^{-6}$ SI) from the south-west coast of South Africa. Cores GeoB20629-1 and 20628-1 from the south coast exhibit also relatively low mean magnetic susceptibilities (42 and 89 $\cdot 10^{-6}$ SI, respectively). Higher values represent the expected fluvial fluxes in south-eastern Indian Ocean. Whether the higher values in the top most layers for cores GeoB20620-4 (up to $4200 \cdot 10^{-6}$ SI) from the Natal Valley and GeoB20608-1 (up to $3000 \cdot 10^{-6}$ SI) from the Limpopo area are coring artifacts is not yet clear. High absolute numbers of magnetic susceptibility with relatively low variability expressed as standard deviation were found for cores GeoB20607-2 and GeoB20609-2. This indicates continuously high supply of terrigenous material at these locations, which are most distant from the Limpopo River mouth compared to other coring sites in this area.

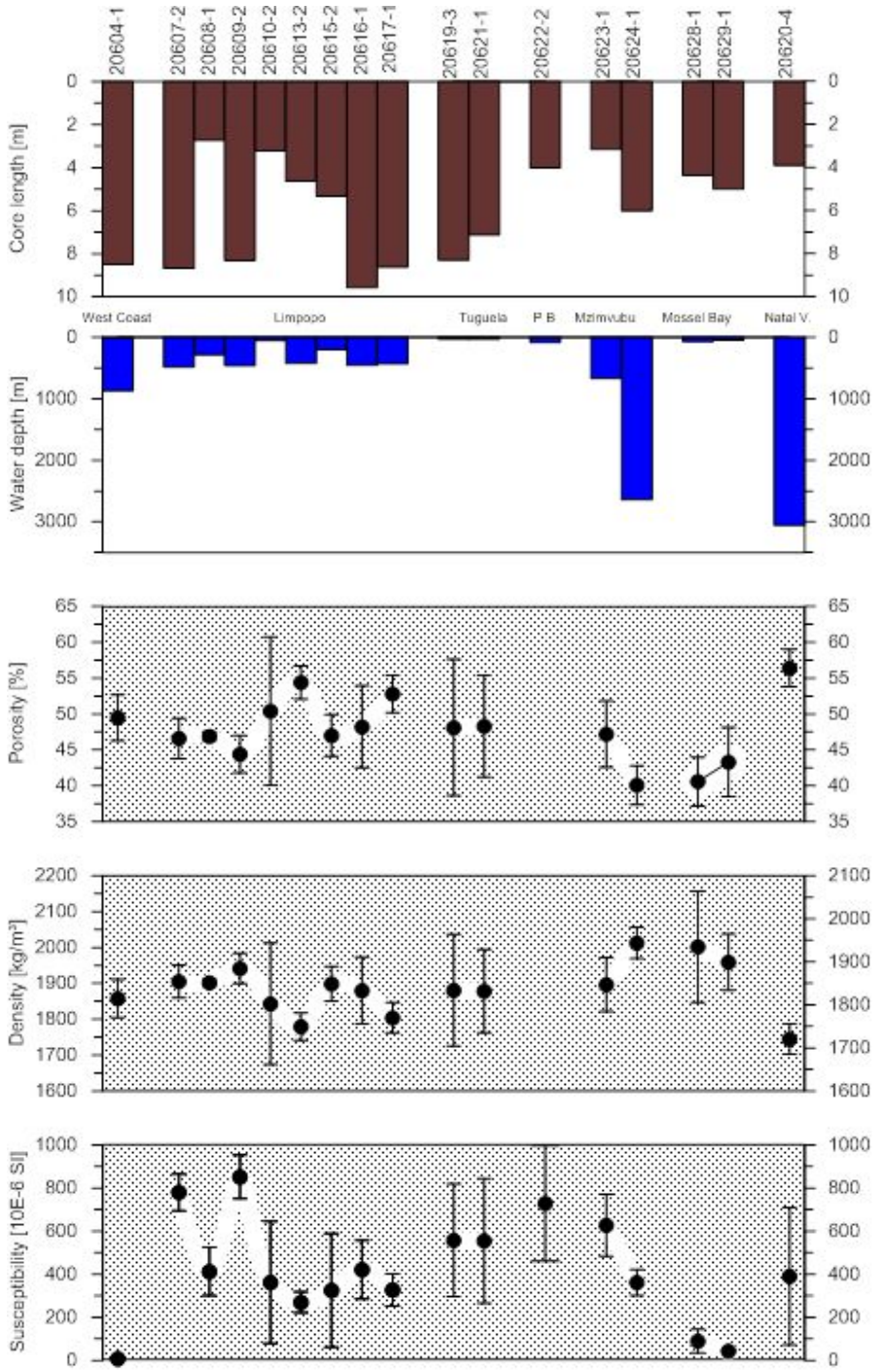

Fig. 4.9

Core length, water depth, mean porosity, density, and magnetic susceptibility of all M123 cores. Vertical error bars denote standard deviations.

Core images and reflectance data (see Figs. 4.13 – 4.16) document generally medium dark greyish-greenish sediment colors for all cores from the Limpopo area (GeoB20607-2, 20608-1, 20609-2, 20610-2, 20613-2, 20615-2, 20616-1, 20617-1) with average L* values of about 40–45%. In contrast, cores GeoB20621-1 and 20623-1 from more southerly locations off the Tugela and Mzimvubu Rivers, respectively, comprise of darker colors with mean L* values of around 30%. Cores from deeper water depths (GeoB20620-4, GeoB20624-1) exhibit greater light reflectance at least in the upper brownish part (GeoB20620-4). This was seen through the whole sediment sequence recovered (GeoB20624-1). Both these cores consist of a more greenish lithology from the middle to lower parts. Furthermore, the latter parts of both cores show more pronounced and almost cyclic behavior of high and low light reflectances. Although from a completely different depositional environment, core GeoB20601-4 shows similar alternations of

high and low reflectivity and red-blue ratios. This is seen to be a lot less variable for the cores from the east coast of southern Africa. Core GeoB20622-2 is sandier and shows more yellowish colors. This color continues down to a core depth of 3 meters, with higher reflectivity and mean L* values of approximately 55%.

West Coast (core GeoB20601-4):
This core shows cyclic behavior around mean values without any trend in color related parameters, porosity and magnetic susceptibility. The absolute values of magnetic susceptibility are the lowest of all the cores recovered during the cruise. This points to a very limited influx of terrigenous material and/or dilution by high amounts of biogenic material. Porosity is almost equal to the cores from the eastern coast of South Africa. The core with relatively high color reflectance displays a high red-blue ratio of about 1.6 and up to 1.8 in the upper meter. This indicates an enhanced content of reddish minerals, probably hematite particles transported by wind.

Limpopo River area (cores GeoB 20607-2 through 20617-1):
This group of cores can be subdivided in three subgroups based on similar patterns of magnetic susceptibility: group 1 consists of cores GeoB20607-2, 20608-1 and 20609-2 with GeoB20607-2 being the stratigraphically oldest core (Fig. 4.10); group 2 comprises cores GeoB20613-2, 20616-1 and 20617-1 with GeoB20617-2 reaching most far back into time (Fig. 4.11). The cores of the third subgroup, GeoB20610-2 and 20615-2, show almost no common features and thus seem to represent different depositional conditions compared to all other sediment cores from this area.

These cores were taken from water depths between 59 and 485 m, they show low red-blue ratios of about 1.2 which can increase up to 1.7 in the upper 50 cm of sediment. These increases indicate more oxic conditions. Porosity and magnetic susceptibility vary for all cores by a factor greater than two. The optical parameters show lower variability with the exception of core GeoB20617-1. The color reflectance L* of the latter varies between about 40% and more than 65% with a semi-cyclic character.

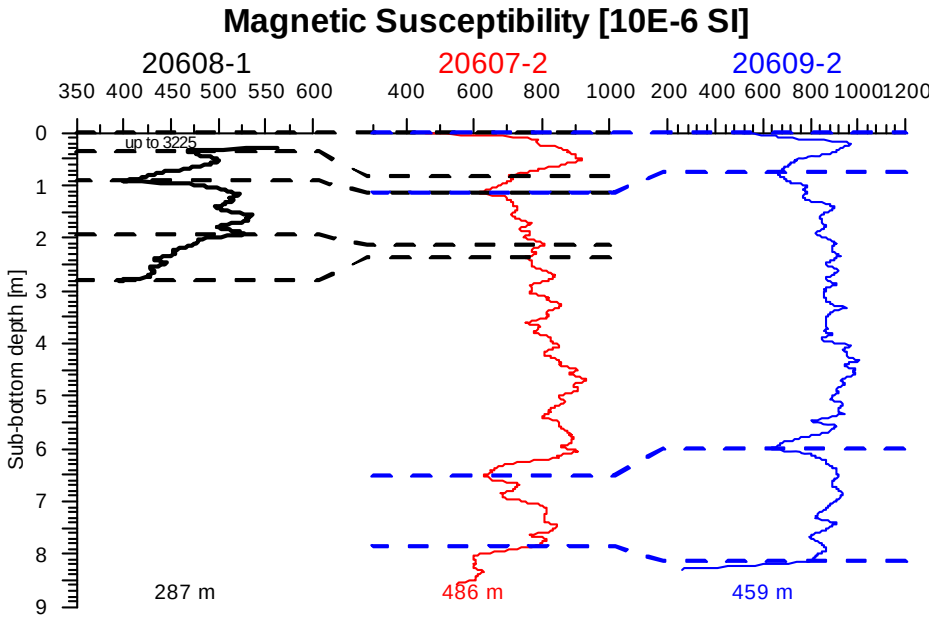

Fig 4.10

Magnetic susceptibility of gravity cores GeoB 20607-2, 20608-1 and 20609-2 from the Limpopo area. Dashed lines indicate tentative correlation tie points.

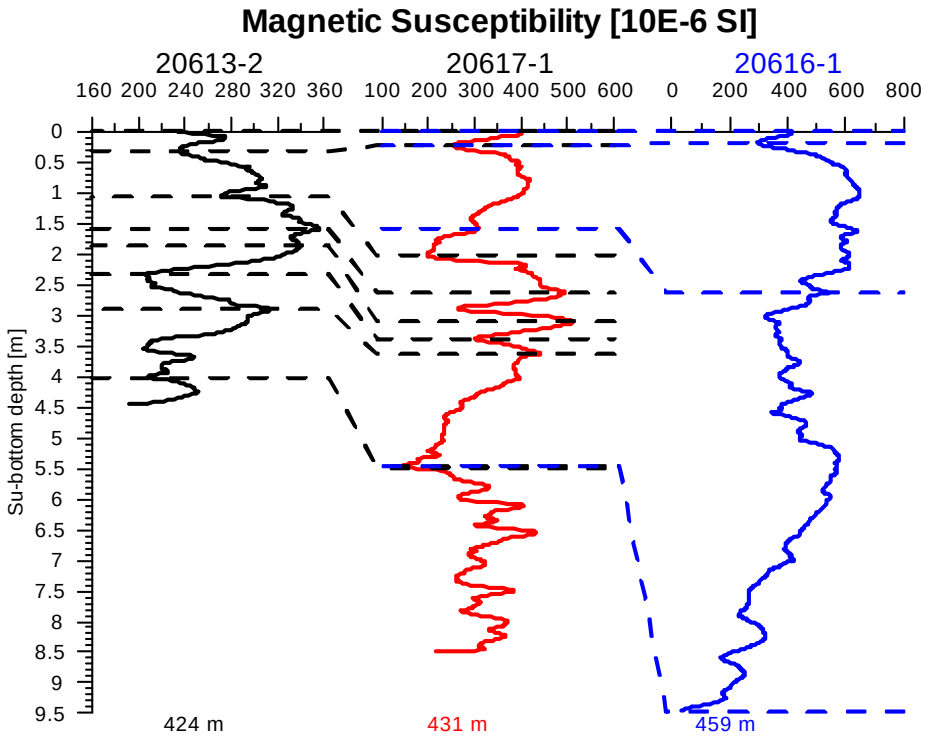

Fig 4.11

Magnetic susceptibility of gravity cores GeoB 20613-2, 20616-1 and 20617-1 from the Limpopo area. Dashed lines indicate tentative correlation tie points.

Tugela River area (cores GeoB20619-3 and 20621-2):

Core GeoB20621-1 and GeoB20619-3 demonstrate very similar variations and were recovered from almost identical water depths of 32 and 34 m at almost the same site location. GeoB20621-1 consists of relatively dark sediments showing a mean color reflectance L* of about 30% in the upper 3 m and 20% in deeper strata. Red-blue ratios are also low with a mean value of about 1. Relatively high porosities of greater than 60% decreases with a linear trend to about 40% at the core base. Magnetic susceptibility shows low variability down-core with a mean of $555 \cdot 10^{-6}$ SI and a prominent peak of up to $2600 \cdot 10^{-6}$ SI at a core depth of ~7 m. The magnetic susceptibility signal of core GeoB20621-1 can be easily correlated to that of core GeoB20619-3 (Fig. 4.12). This correlation shows that core GeoB20619-3 loses a part of the topmost sediment layers but cored stratigraphically older horizons at the bottom. Both these cores showed the highest variability of all the cores in each physical parameter.

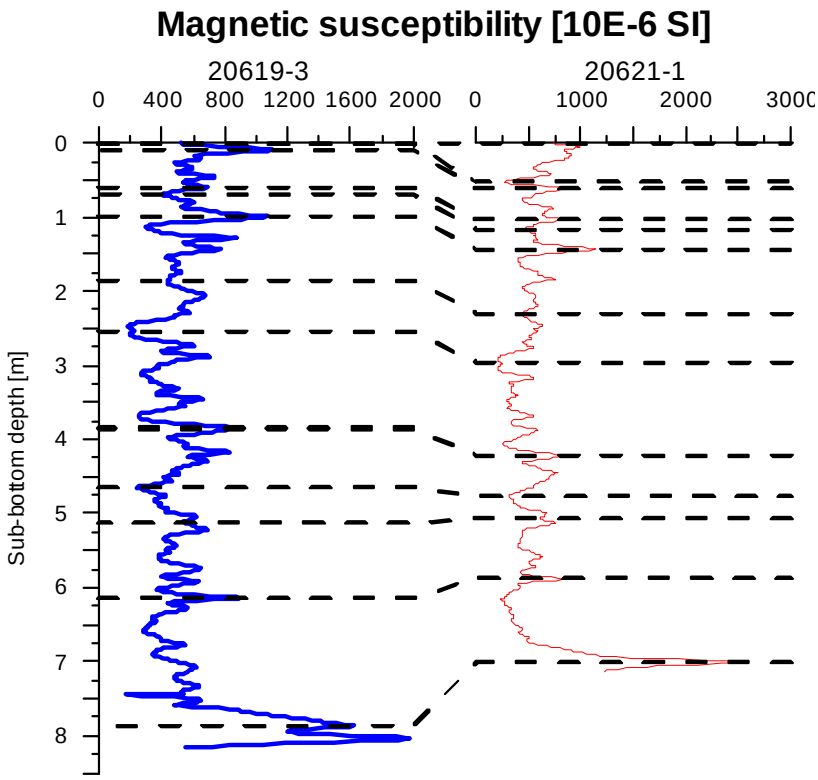

Fig. 4.12

Magnetic susceptibility of gravity cores GeoB 20619-3 and 20621-1 from the Tugela area. Dashed lines indicate tentative correlation tie points.

Natal Valley / Deep Agulhas (core GeoB20620-4):
This core was recovered from a water depth of 3059 m and exhibits a significant color change at about 0.5 m core depth from bright yellow colors to darker greenish colors. Color reflectance L* decreases from 80% to 40%. Parallel with the color change the red-blue ratio decreases from values of ~1.7 to 1.2. Porosity shows a slight cyclic behavior that seems to be, at least partly, related to the fluctuations of color reflectance. Magnetic susceptibility shows a similar pattern but with less pronounced variations. At the top of the sediment core, magnetic susceptibility reaches the highest value of all the cores with a value of up to $4200 \cdot 10^{-6}$ SI. Whether this value is realistic or due to coring artifacts is still unknown.

Protea Banks (core GeoB20622-2):
This vibro core was recovered from a water depth of about 85 m and shows one of the highest mean magnetic susceptibilities of all cores ($729 \cdot 10^{-6}$ SI) with a significant increase at a core depth of about 1.5 m. The variability of magnetic susceptibility is the highest among all the cores indicating variable depositional conditions. The upper 3 m show a relatively high color reflectance with a mean L* of about 55% which then decreases to medium values of about 45%. The red-blue ratio also exhibits high values (up to around 2) which decrease to values of around 1.5 at a depth of about 3 m.

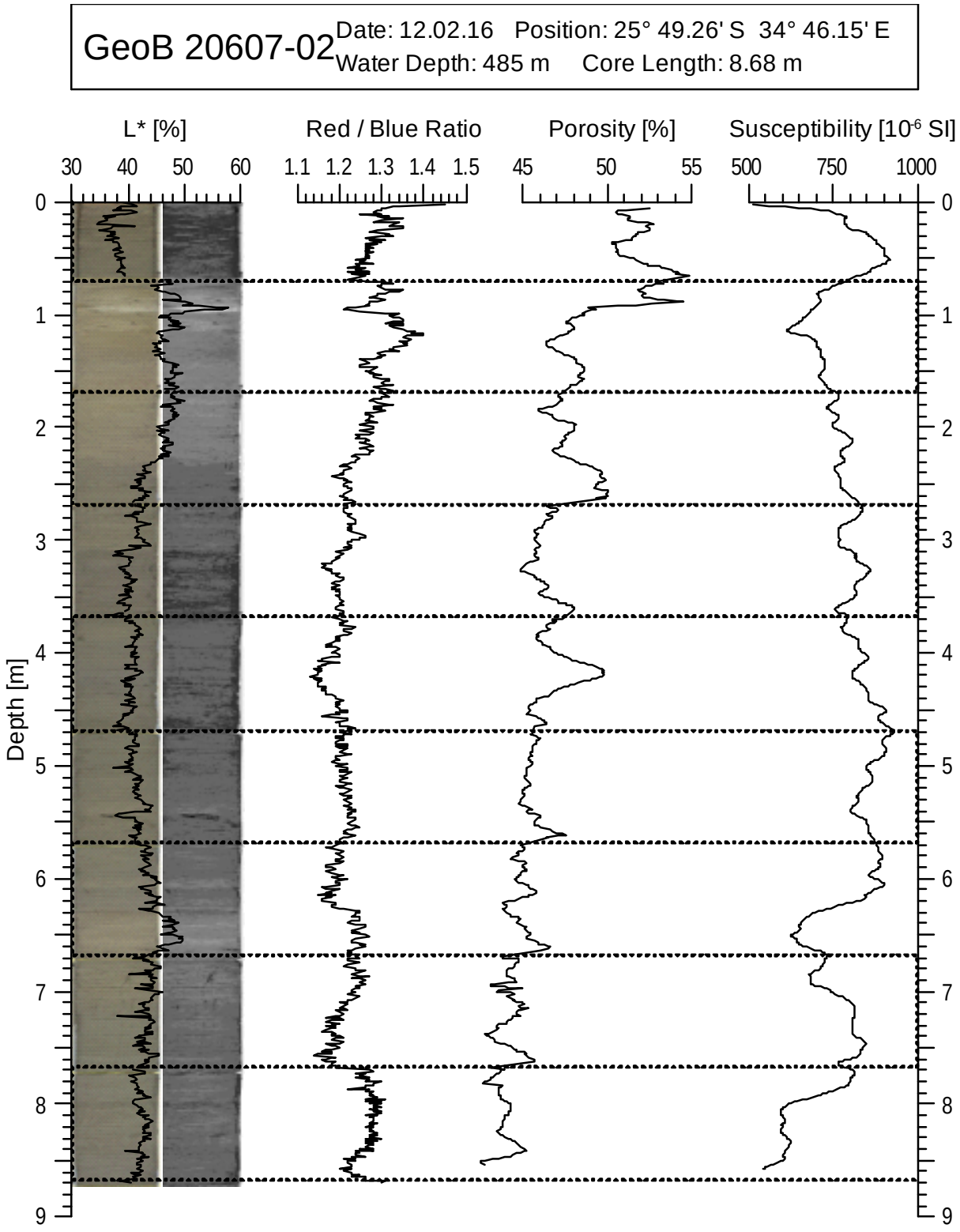

Fig. 4.13 Optical parameters (color reflectance L*, red-blue ratio) and physical properties of gravity core GeoB20607-2 from Limpopo River area.

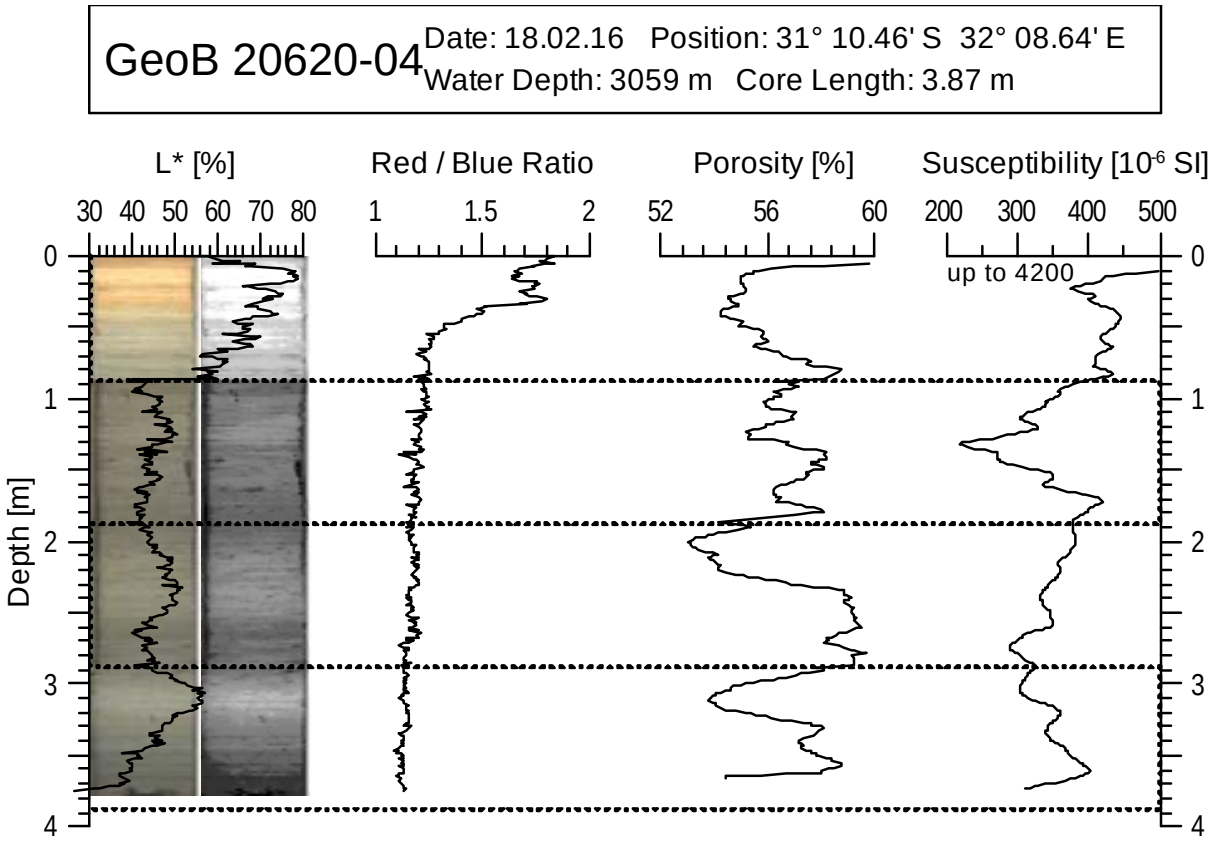

Fig. 4.14 Optical parameters (color reflectance L*, red-blue ratio) and physical properties of gravity core GeoB20620-4 from Deep Agulhas.

Mzimvubu River and Mzimvubu Canyon (cores GeoB20623-1 and 20624-1):
These two cores were recovered in front of the mouth of the Mzimvubu River and the Mzimvubu Canyon and stem from significantly different water depths of 671 m (GeoB20623-1) and 2644 m (GeoB20624-1), respectively. Thus they represent different deposition regimes. While core GeoB20624-1 shows mostly bright greenish and yellow colors at the topmost 25 cm, core GeoB20623-01 and GeoB20621-1 from the Tugela River area show the darkest colors of all the cores recovered with a very low color reflectance of 20 to 30%. Furthermore core GeoB20624-1 exhibits the highest mean density of ~2012 kg/m³ of all the gravity cores. Most of the parameters, including L*, density and magnetic susceptibility show cyclic behavior suggesting that this core from relatively deep water depth may have records glacial-interglacial cycles.

Breede River area and Mossel Bay (cores GeoB20628-1 and 20629-1):
These two cores show the lowest magnetic susceptibility of all cores recovered at the eastern and southern coast (means 89 and $42 \cdot 10^{-6}$ SI, respectively). While core GeoB20628-1 shows a moderate color reflectance of around 40% with an almost constant red-blue ratio of 1.4 which can increase to values up to 2.1 for core depths greater than 3 m, core GeoB20629-1 exhibits higher red-blue ratios for the top most 1.5 m which decrease to values of ~1.1 down-core. Its color reflectance shows a trend to higher values down-core. The red-blue ratio of core GeoB20628-1 varies almost parallel with magnetic susceptibility which is low and almost constant in the upper 2.5 m and increases by a factor of 2 for the lower sediments. For porosity, the two cores show opposite trends. While in core GeoB20628-1 porosity decreases from high values of ~70% to low 30% down-core, the values increase from 30% to 40% in the upper 4 m of core GeoB 20629-1 and decrease again further down.

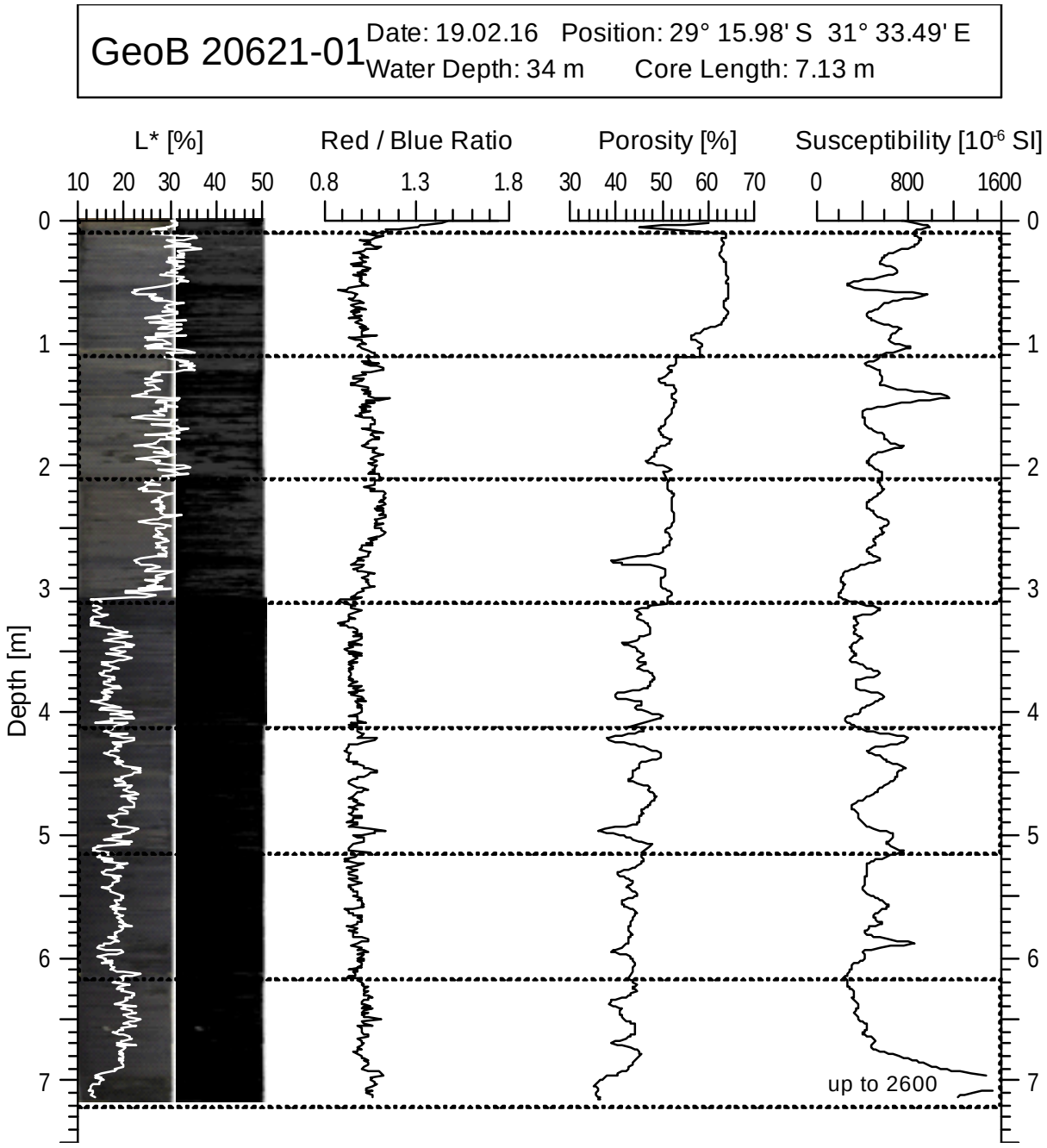

Fig. 4.15 Optical parameters (color reflectance L*, red-blue ratio) and physical properties of gravity core GeoB20621-1 from Tuguela River area.

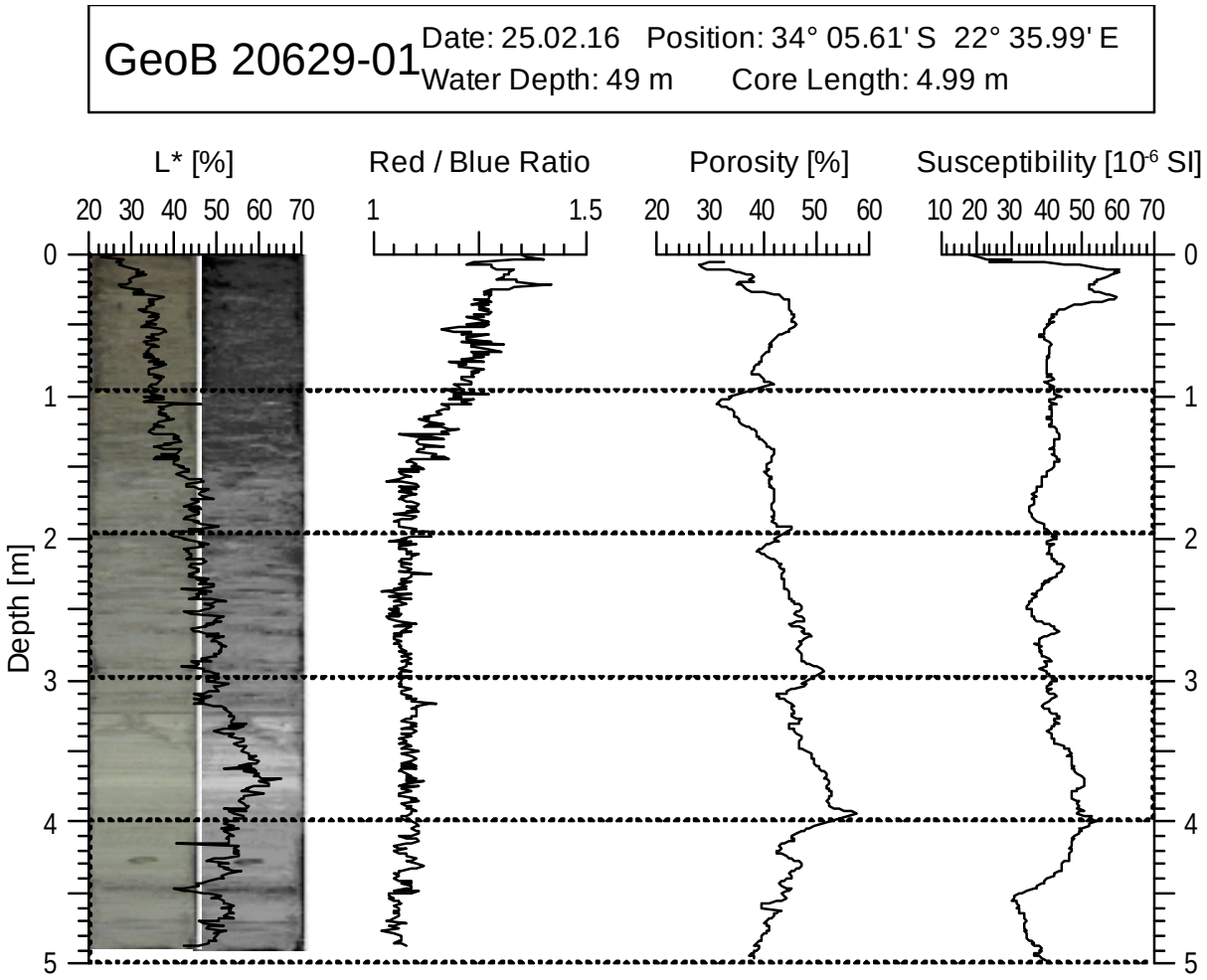

Fig. 4.16 Optical parameters (color reflectance L*, red-blue ratio) and physical properties of vibro core GeoB20629-1 from Mossel Bay.

4.4 Mineralogy

(S. Andó)

Reconstructing the erosion of the eastern passive margin of Africa is a key goal of R/V METEOR expedition M123, consequently we need to distinguish sediment delivered from different rivers and their erosional and dispersal pattern under the influence of the Agulhas current along the shelf. Some of this work requires shore-based provenance studies coupling different bulk methods (petrography; geochemistry) and single grain methods (heavy-mineral; zircon age; Raman spectroscopy), but initial mineralogical studies on board are able to pinpoint the contribution of different rivers using traditional microscopy applied to heavy minerals in smear slides.

4.4.1 Methods

Semi-quantitative studies of the mineralogy of sand to silt size sediments were conducted on board of the Meteor during expedition M123 using a monocular polarizing microscope Carl Zeiss with 10x, 40x objectives. Classical methods following the "Book" of Mange & Maurer, 1992, where applied to identify different varieties of heavy minerals. Working with students on board, a table of properties and photos of all the minerals encountered were prepared to facilitate the proper identification of the heavy mineral suite in different samples. The light fraction

comprising detrital light minerals and biogenic fragments represents the highest percentage of the sediment by composition. We have thus also considered these grains in the table so as to complete the catalogue of detrital minerals.

Smear slides were prepared using two different procedures. To better identify the grain size, and to correctly identify single sedimentary layers, a proper smear slide was prepared by spreading a small amount of sediment on the slide with water. After drying, a few drops of Norland 61 (n=1.54) were added and the slide fixed with a portable UV light.

The second procedure is modified for semi-quantitative heavy-mineral analysis on board and serves to separate the clay fraction from the sediment. Samples were washed by water, taking care to avoid loss of the pure sand and silt into the sink. The adopted procedure allows us to better identify heavy minerals with the polarizing microscope and it eliminates most of the aggregates of minerals and organic matter, micritic cement and nannofossil muds. A clean smear slide with heavy grains is ready for grain counting. To speed up the process of counting heavy minerals on board, and because the number of heavy grains is significantly less than the light and biogenic fractions, the counting technique "area method" (Mange & Maurer, 1992) was used. Only transparent and opaque heavy minerals, Ti-oxides, Fe-oxides, glaucony, chlorite, biotite, authigenic carbonate in euhedral crystals were counted. In this study of the mineralogy of Southern Africa sediments we have distinguished minerals in the silt to sand grain size window. These were: zircon, tourmaline, rutile, titanite, apatite, hornblende, actinolite, augite, diopside, enstatite, hypersthene, spinel, epidote, zoisite, allanite, pumpellyite, chloritoid, garnet, staurolite, andalusite, kyanite, sillimanite. For each group of minerals we have also described the color to distinguish varieties. Surficial features of each single grain were also examined to investigate the possible link between climate and weathering encoded on each single mineral. In particular pyroxenes and amphiboles develop sharp corrosion features, displaying typically from corroded to etched and skeletal outlines. It is possible to quantify these characteristics applying a visual classification proposed in a catalogue of corrosion features by Andó et al. (2012).

4.4.2 Mineralogical suite of heavy-minerals in different working areas

A total amount of 125 samples were collected for onshore heavy mineral and bulk petrography quantitative analyses for provenance studies. 48 smear slides were prepared and analyzed on board for heavy mineral semi-quantitative studies and to identify different sources of the detrital input and their dispersal in the marine environment (Tab. 4.1).

Bay of Maputo:

A total of 28 smear slides were prepared from this working area 1 and 14 were analyzed for the heavy mineral suite. These ranged from sand to fine silt grain size. In surficial sediments, moving from the mouth of the Limpopo River to East and in a clockwise direction, following the main current patterns in the Bay of Maputo, we recognize in samples GeoB20610; 20609; 20607 a similar assemblage with a moderate to rich amount of heavy minerals, abundant amphibole, 32-39% and epidote, 22-31%, very common clinopyroxene, 13-25%, subordinate garnet, 3-7 %, and zircon, tourmaline, rutile (ZTR), 2-7%, with minor orthopyroxene (1-4%) and other heavy minerals (&HM) 1-3%. Sample GeoB20615 is west of the mouth of the Limpopo River and closer to the shoreline and it contains a low amount of HM with a very different mineral suite, probably influenced by the erosion and contribution of the aeolian dunes of Maputo. Epidote is abundant, 33%, with clinopyroxene, 28%, amphibole is common 15%, zircon represents 9%

Table 4.1

Site	Type	Section cm	depth cm	SS	W SS	% HM	Zrn	Tou	Rt	Ttn	Ap	Hbl	Act	MRF Amp	Aug	Di	& Cpx	En	Hy	Sp	Ep	Zo	MRF Ep	Grt	MM	& HM	Tot tHM	Op	Fe ox	Ti ox	Gla	Chl	Bt br	Bt gr	Cal	Tot op&	Tot counted
GeoB 20607_1	MC		2–4	N	Y	H	8	0	4	0	1	41	14	0	7	16	20	1	7	0	37	1	0	12	1	1	171	71	1	0	7	8	1	1	5	94	265
GeoB 20607_1	*MC*		2–4	*N*	*Y*	H	*5*	*0*	*2*	*0*	*1*	*24*	*8*	*0*	*4*	*9*	*12*	*1*	*4*	*0*	*22*	*1*	*0*	*7*	*1*	*1*	*100*	*27*	*0*	*0*	*3*	*3*	*0*	*0*	*2*	*35*	%
GeoB 20607_2	GC	267-367	SS 40	Y	N	M	1	0	5	0	0	44	12	0	0	24	4	3	2	0	35	0	0	0	1	0	131	89	1	1	0	13	4	0	0	108	239
GeoB 20607_2	*GC*	*267-367*	*SS 40*	*Y*	*N*	*M*	*1*	*0*	*4*	*0*	*0*	*34*	*9*	*0*	*0*	*18*	*3*	*2*	*2*	*0*	*27*	*0*	*0*	*0*	*1*	*0*	*100*	*37*	*0*	*0*	*0*	*5*	*2*	*0*	*0*	*45*	%
GeoB 20608_2	MC		2–4	N	Y	M	2	0	1	2	0	12	2	0	0	7	0	0	4	0	16	0	0	3	0	0	49	19	0	1	92	1	3	0	0	116	165
GeoB 20608_2	*MC*		*2--4*	*N*	*Y*	M	*4*	*0*	*2*	*4*	*0*	*24*	*4*	*0*	*0*	*14*	*0*	*0*	*8*	*0*	*33*	*0*	*0*	*6*	*0*	*0*	*100*	*12*	*0*	*1*	*56*	*1*	*2*	*0*	*0*	*70*	%
GeoB 20608_1	GC	192-292	50	Y	N	H	7	0	2	1	0	18	9	0	1	27	1	0	6	1	33	0	0	7	0	0	113	73	3	0	42	33	6	5	7	169	282
GeoB 20608_1	*GC*	*192-292*	*50*	*Y*	*N*	H	*6*	*0*	*2*	*1*	*0*	*16*	*8*	*0*	*1*	*24*	*1*	*0*	*5*	*1*	*29*	*0*	*0*	*6*	*0*	*0*	*100*	*26*	*1*	*0*	*15*	*12*	*2*	*2*	*2*	*60*	%
GeoB 20609_1	MC		2–6	N	Y	M	2	0	0	0	0	28	18	0	2	16	9	0	3	0	31	1	4	3	0	1	118	19	1	1	5	6	3	1	2	38	156
GeoB 20609_1	*MC*		*2--6*	*N*	*Y*	*M*	*2*	*0*	*0*	*0*	*0*	*24*	*15*	*0*	*2*	*14*	*8*	*0*	*3*	*0*	*26*	*1*	*3*	*3*	*0*	*1*	*100*	*12*	*1*	*1*	*3*	*4*	*2*	*1*	*1*	*24*	%
GeoB 20609_2	GC	cc	5-/10	N	Y	L	1	1	1	0	1	37	19	1	2	17	0	0	4	1	25	0	5	5	0	2	122	6	1	2	1	18	11	15	1	55	177
GeoB 20609_2	*GC*	*cc*	*5-/10*	*N*	*Y*	*L*	*1*	*1*	*1*	*0*	*1*	*30*	*16*	*1*	*2*	*14*	*0*	*0*	*3*	*1*	*20*	*0*	*4*	*4*	*0*	*2*	*100*	*3*	*1*	*1*	*1*	*10*	*6*	*8*	*1*	*31*	%
GeoB 20610_2	GC	0-21	5	N	Y	H	5	2	3	1	2	42	24	0	2	8	12	0	2	0	52	0	0	12	0	1	168	55	2	0	0	24	1	13	3	98	266
GeoB 20610_2	*GC*	*0-21*	*5*	*N*	*Y*	H	*3*	*1*	*2*	*1*	*1*	*25*	*14*	*0*	*1*	*5*	*7*	*0*	*1*	*0*	*31*	*0*	*0*	*7*	*0*	*1*	*100*	*21*	*1*	*0*	*0*	*9*	*0*	*5*	*1*	*37*	%
GeoB 20610_2	GC	121-221	78–80	N	Y	H	7	1	0	1	2	31	13	0	3	20	16	0	14	0	25	2	0	12	0	1	148	70	0	2	16	25	1	1	4	119	267
GeoB 20610_2	*GC*	*121-221*	*78--80*	*N*	*Y*	H	*5*	*1*	*0*	*1*	*1*	*21*	*9*	*0*	*2*	*14*	*11*	*0*	*9*	*0*	*17*	*1*	*0*	*8*	*0*	*1*	*100*	*26*	*0*	*1*	*6*	*9*	*0*	*0*	*1*	*45*	%
GeoB 20611_1	BC		0–3	N	Y	H	2	0	0	2	1	29	9	1	1	17	7	2	11	1	25	1	0	5	1	1	116	97	0	0	1	1	1	0	0	100	216
GeoB 20611_1	*BC*		*0--3*	*N*	*Y*	H	*2*	*0*	*0*	*2*	*1*	*25*	*8*	*1*	*1*	*15*	*6*	*2*	*9*	*1*	*22*	*1*	*0*	*4*	*1*	*1*	*100*	*45*	*0*	*0*	*0*	*0*	*0*	*0*	*0*	*46*	%
GeoB 20615_2	GC	0-31	16–18	N	Y	L	6	0	0	0	0	6	4	0	2	14	3	0	3	0	22	0	0	4	3	0	67	7	0	0	3	1	0	0	6	17	84
GeoB 20615_2	*GC*	*0-31*	*16--18*	*N*	*Y*	*L*	*9*	*0*	*0*	*0*	*0*	*9*	*6*	*0*	*3*	*21*	*4*	*0*	*4*	*0*	*33*	*0*	*0*	*6*	*4*	*0*	*100*	*8*	*0*	*0*	*4*	*1*	*0*	*0*	*7*	*20*	%
GeoB 20615_2	GC	cc	0–5	*N*	*Y*	M	4	1	1	1	0	24	24	0	3	17	4	0	1	1	32	1	0	5	0	4	123	40	2	6	7	17	12	1	23	108	231
GeoB 20615_2	*GC*	*cc*	*0--5*	*N*	*Y*	M	*3*	*1*	*1*	*1*	*0*	*20*	*20*	*0*	*2*	*14*	*3*	*0*	*1*	*1*	*26*	*1*	*0*	*4*	*0*	*3*	*100*	*17*	*1*	*3*	*3*	*7*	*5*	*0*	*10*	*47*	%
																																					2348

H	rich HM %	H	Zircon (Zrn), Tourmaline (Tou), Rutile (Rt), Titanite (Ttn), Apatite (Ap), Hornblende (Hbl), Actinolite (Act), Metamorphic rock fragments with amphibole (MRF Amp),
M	moderate HM %	M	Augite (Aug), Diopside (Di), Other Cpx (&Cpx), Enstatite (En), Hypersthene (Hy), Spinel (Sp), Zoisite (Zo), Metamorphic rock fragments with Epidote (MRF Ep),
L	poor HM %	L	Garnet (Grt), Metamorphic minerals like sillimanite, kyanite andalusite, staurolite (MM), Others HM (&HM), Opaque (Op), Iron-oxides (Fe-ox), Titanium-oxides (Ti-ox), Glaucony (Gla), Chlorite (Chl), brown Biotite (Bt br), green Biotite (Bt gr), Calcite (Cal).

GeoB 20604_1	BC			N	Y	ML	7	3	8	2	1	27	14	0	3	26	34	0	0	0	18	0	0	12	0	0	155	67	3	3	0	13	3	8	2	99	254
GeoB 20604_1	*BC*			*N*	*Y*	ML	*5*	*2*	*5*	*1*	*1*	*17*	*9*	*0*	*2*	*17*	*22*	*0*	*0*	*0*	*12*	*0*	*0*	*8*	*0*	*0*	*100*	*26*	*1*	*1*	*0*	*5*	*1*	*3*	*1*	*39*	

(aeolian contribution), minor garnet 6%, orthopyroxene 4% and &HM 4%. GeoB20616 is a transitionary or intermediary sample from the central gyre of the Bay; 20617; 20613; 20608 are characterized by a very poor assemblage of HM and enriched in forams, biogenic debris and glaucony within the central part of the current gyre circulation. GeoB20616 contains low amounts of HM with common epidote, amphibole and clinopyroxene, rare zircon and tourmaline and trace of apatite, garnet and orthopyroxene. GeoB20617; 20613; 20608 contain very rare or trace of HM with amphibole and clinopyroxene. In the deeper samples we have a similar trend; concentrations of heavy minerals but differences among samples in the same core are possible and further quantitative analyses are indispensable for a proper discussion.

Tugela Mouth area:

7 smear slides from working area 2 were analyzed. All these samples display poor assemblages of heavy minerals with few varieties. GeoB20620-4 contains low amounts of garnet, epidote, diopside and hornblende. GeoB20619-3 and GeoB20625-1 have very low amounts of HM with epidote, garnet and diopside. GeoB20605-1 contains negligible amounts of hornblende. Fine sand and silt in samples GeoB20604-1, from the area of Port St. Johns and the Mzimvubu River Canyon, contains a medium to rich suite of HM. The assemblage is dominated by the presence of colorless or pale green clinopyroxene 41% (derived mostly from the dolerite dikes), common amphibole (hornblende and actinolite) 26%, frequent epidote 12%, ZTR 12% and garnet 8% and minor &HM. The sample GeoB20602-1 in front of Port Elizabeth contains low amounts of HM with epidote, clinopyroxene, zircon, garnet and glaucony.

Mossel Bay:

GeoB20628 displays recycled sediments from Cretaceous sediments with only minor quantities of HM with abundant zircon and glaucony. GeoB20629 is a fine, well sorted sand, with very low amounts of HM. Common minerals include garnet and subordinate etched clinopyroxenes and unweathered zircon. The only sample collected in the Western Coast of South Africa is GeoB20601-4 which was dominated by biogenic sediments, foraminiferal sand with nannofossils or bioclastic sand with abundant forams and glaucony without undetectable amounts of HM.

4.4.3 Discussion

This heavy mineral assemblage in the Work area 1 in the Bay of Maputo is very similar to the modern Limpopo River composition (Garzanti et al, 2014) but an important contribution from the deflation of the dune field of Maputo is also a possible factor in feeding ultra-stable minerals to the system. The rounded quartz grains are likely to effectively dilute the amount of pyroxene derived from the Olifants to the Limpopo River. The high content of amphiboles provided by Kapvaal and Zimbabwe Cratons could be affected by the local gyre circulation in the Bay of Maputo, where sediments from the Limpopo River are entrained in the SE to NE current with an accumulation of ultra-dense zircon and garnet in sample GeoB20610 and an increasing amount of hornblende in samples 20609 and 20607. In this trajectory, sediments poor in heavy minerals reach the area marked by samples 20615 and 20616 where a SE contribution from the offshore deflation of coastal dunes adds abundant quartz and zircon. The central area of the gyre system is a relatively high productivity zone with very abundant biogenic fractions and very poor heavy minerals content (dilution effect). Furthermore, a strong link to the Limpopo River is demonstrated by the presence of amphibole and epidote derived from the continental block of the old cratons, and pyroxene, with a marker-mineral, the green-pink hypersthene derived from the

erosion of the Bushveld Complex and carried by the Olifants a tributary of the Limpopo River to the marine environment.

The adopted "area method" could affect the described percentages of heavy minerals and a "point counting" method is advisable for a quantitative analysis to be conducted onshore (Galehouse, 1971). In this light, epidote could be overestimated because in marine samples it is usually smaller than amphiboles and pyroxenes. Corrosion features are very common on pyroxenes and less common on amphiboles and epidotes, so we have to take into account a possible surficial weathering effect on the observed suites of heavy minerals. This is possible after weighing the HM fraction in the laboratory for provenance studies of Milano-Bicocca, Italy after onshore heavy mineral gravimetric separations.

The relative abundance of different heavy minerals in a quantitative study is possible, comparing our newly collected data set with the modern dataset on land (as published in previous studies) and future analyses on additional samples collected in the Limpopo catchment during previous MARUM expeditions.

4.5 Microfossils

(P. Frenzel, E. Bergh, L. Gander, K. Strachan)

The sampling and preliminary analysis of microfossils sampled during R/V METEOR Cruise M123 had two main objectives; 1) the documentation of recent fauna, focusing primarily on Foraminifera and Ostracoda, thus developing taxonomic reference material and ecological/distribution data as a base for later analysis of fossil material from marine sediment cores, and 2) preliminary descriptions of associations from extracted cores, providing an overview on the general distribution patterns (abundances, P/B ratio), maximum ages of cores relying on biostratigraphical analysis and first insights into depositional environments by palaeoecological interpretation. Macrofossil extracted from sediment cores during the documentation by other working groups were identified and an interpretation given.

4.5.1 Methods

All core and surface samples were wet sieved using seawater through a 63 µm and 1000 µm sieve, separating the bigger components from the smaller components. Sieved surface samples were examined under a binocular microscope for both living ostracods and foraminifera. Living ostracods were collected and stored separately in ethanol, while living foraminiferal specimens were dried. A short documentation and description of each sample was compiled before adding Rose Bengal to each surface sample to stain the soft parts of any living foraminifera. Following this step samples were dried in an oven at 60°C.

4.5.2 Description of Surface Samples

The following descriptions are based on the visual inspection of the surface sediments in each of the box cores and multi-cores, and on qualitative microscopical observations of sieved sediment samples (>63 µm). See Figure 3.1 for positions of sampling stations. A remarkable observation was the generally abundant presence of glauconite in foraminifera tests from the upper slope.

<u>GeoB20602-1:</u>
Habitat: green mud, no anoxic layer visible, faecal pellets and some black concretion of mm-scale, rare glauconite

Fauna: some tubes of crayfish, shell detritus and Scaphopoda, rich foraminifera fauna (*Ammonia*, *Elphidium*, *Amphicoryna*, *Cassidulina*, *Miliolids*, *Lagena*, rare planktonic foraminifera), rich ostracod fauna (two alive), fragments of Mollusca, Bryozoa and Echinodermata
Interpretation: well preserved recent inner shelf soft bottom association on older (Pleistocene?) sediments

Fig. 4.17 Sieved surface sample in BC GeoB20602-1 (>63 µm)

GeoB20603-1:

Habitat: carbonate sand, surface well-oxygenated, coarse sand with larger shell fragments, 90 % biogenic fragments, 10 % moderately rounded quartz

Fauna: fragments of Mollusca, Bryozoa and Echinodermata, well preserved foraminifera (miliolids, *Elphidium*, *Lenticulina*, *Lobatula*, rare *Ammonia*, *Amphicoryna* and planktonic foraminifers), only a few living animals (*Amphipoda* and fixosessile foraminifera)
Interpretation: sorted shell accumulation, mostly allochthonous, turbulent water

Fig. 4.18 Sieved surface sample in BC GeoB20603-1 (>63 µm)

GeoB20604-1 (off Mzimvubu River):

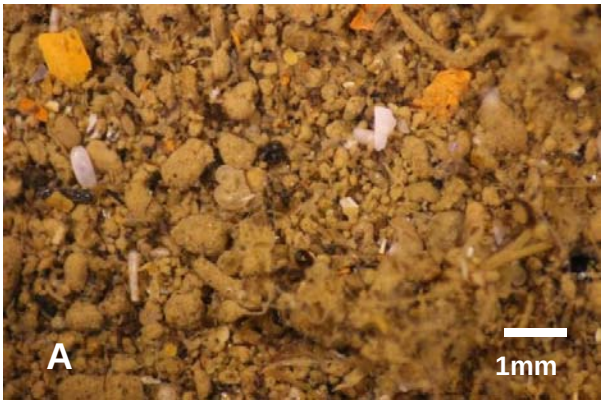

Habitat: green to brown mud, oxygenated, little agglutinated tubes at the surface, faecal pellets, rich in organic detritus.
Fauna: diverse benthic and planktonic foraminiferal species (large agglutinated forms: *Reophax*, *Rhabdammina* (mm-scale), mioliolids, lagenids), rare Ostracoda, mostly dead, only a few living individuals, Crustacea and worms, juvenile shells, many Radiolaria.
Interpretation: autochthonous bathyal association from a submarine canyon, bottom current indicated by filter feeders.

Fig. 4.19 A) Sieved surface sample in BC GeoB20604-1 (>63 µm); B) Large elongated agglutinated foraminifers *Rhabdammina*(?)

GeoB20605-1 **(**off Tugela River):
Habitat: brown sand, well sorted, very coarse, well oxygenated, subangular to angular quartz, feldspar, rock fragments and blackish concretions
Fauna: low proportion of biogenic material, low diverse fauna, reworked biogenic material, some well-rounded, no planktonic foraminifera, some benthic foraminiferal species (*Ammonia*, miliolids, polymorphinids), juvenile shells and corals, fragments of Mollusca, Bryozoa, Echinodermata and Balanidae, no Ostracoda, some Scaphopoda, some snails, one living ophiuroid
Interpretation: well sorted littoral sand

Fig. 4.20
Sieved surface sample in BC GeoB20605-1 (>63 µm)

GeoB20607-1 **(**Limpopo fan):
Habitat: foraminiferal ooze, sand with low proportion of detritus, clay intraclasts, angular quartz, small blackish concretions, glauconite
Fauna: microfossils and macrofossils (solitary corals, Echinodermata, Balanidae, benthic and planktic Gastropoda, bivalves, Bryozoa), mollusk fragments, planktic foraminifers dominant (globigerinids + *Globorotalia*, *Orbulina*), lagenids (*Laevidentalina*, *Amphicorina* etc.), agglutinated forms, *Quinqueloculina*, *Cibicidoides*, *Bolivina*, *Pyrgo*, few ostracods
Interpretation: bathyal globigerinid ooze, slope association

Fig. 4.21
Sieved surface sample in MC GeoB20607-1 (>63 µm)

GeoB20608-2 **(**Limpopo fan):
Habitat: muddy sand, small proportion of organic detritus, at the surface agglutinated tubes, sand with small blackish concretions, with some foraminiferal grains of glauconite, small subangular quartz
Fauna: rich fauna of planktonic foraminiferal species (globigerinids, *Globorotalia*, *Orbulina*), some taxa of benthic foraminifers (*Cibicidoides*, lagenids (*Laevidentalina*, *Lenticulina*, *Saracenaria*, *Nodosaria*), *Pyrgo*, *Spiroloculina*, many sponge spicules, ostracods are very rare (only one living ostracod)
Interpretation: bathyal globigerinid ooze, slope association

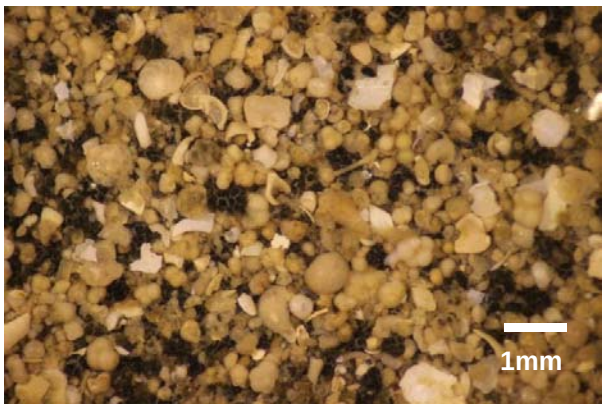

Fig. 4.22 Sieved (>63 µm) surface sample of MC GeoB20608-2

GeoB20609-1 **(**Limpopo fan):

Habitat: sand with low proportion of detritus, small blackish concretions, angular quartz, glauconite

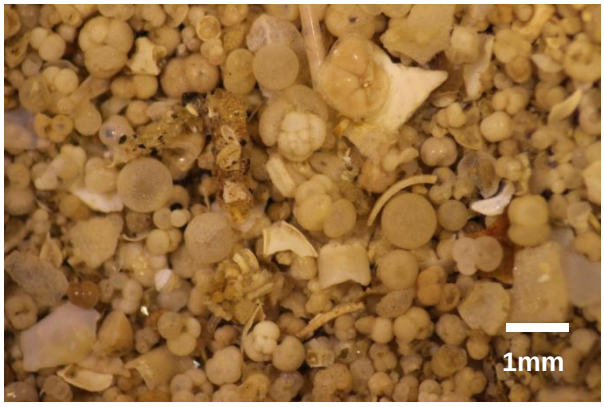

Fauna: fragments of bivalves, Echinodermata, Bryozoa, planktic Gastropods, planktonic foraminifera dominant (globigerinids + *Globorotalia*, *Orbulina*), *Cibicidoides*, lagenids, otoliths, *Spiroloculina*, some agglutinated foraminifera, Scaphopoda, some sponge spicules, and rare ostracods

Interpretation: bathyal globigerinid ooze, slope association

Fig. 4.23 Sieved (>63 µm) surface sample of MC GeoB20609-1

GeoB20610-1 **(**Limpopo fan):

Habitat: greenish brown, sandy mud, fine-grained and well sorted, oxygenated surface (up to 1cm), sand with high proportion of detritus, much more detritus than biogenic minerals, small blackish concretions and many faecal pellets, subangular to angular grains of quartz and feldspar, rock fragments and mica, rare glauconite

Fauna: mud with bivalves, Crustacea, snails, worms and echinoids, polychaets, juveniles and fragments of bivalves, Echinodermata, Bryozoa, rare planktonic foraminiferal species (globigerinids, *Globorotalias*, *Orbulina*), benthic foraminifera (*Ammonia*, *Quinqueloculina*, elphidiids, lagenids (rare), bolivinids), small ostracods (4 living)

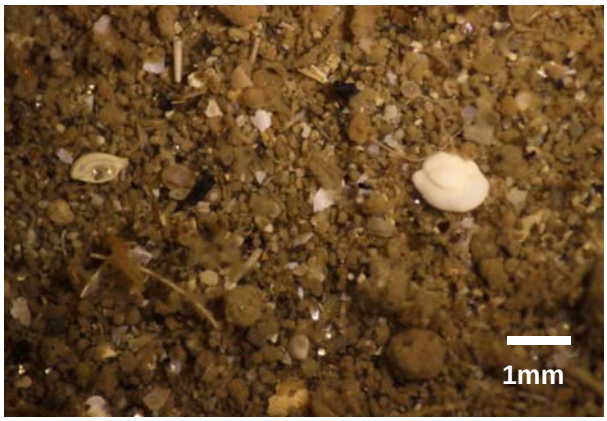

Interpretation: sublittoral habitat with high terrigenic input

Fig. 4.24 Sieved (>63 µm) surface sample in the BC GeoB20610-1

GeoB20611-1 **(**Limpopo fan):
Habitat: brownish green, sandy mud, fine-grained and very well sorted, oxygenated surface, high proportion of detritus, much more detritus than biogenic material, small blackish concretions and many faecal pellets, angular grains of quartz, feldspar and rock fragments, greenish grains are dominant, glauconite
Fauna: fragments of bivalves, Echinodermata, Bryozoa, planktonic foraminifera (globigerinids, *Globorotalia*, *Orbulina*), *Cibicidoides*, lagenids, bolivinids, *Ammonia* (rare), *Lenticulina*, *Spiroloculina*, *Quinqueloculina*, *Dorothia*, many ostracods (7 living)
Interpretation: sublittoral soft bottom association

Fig. 4.25 Sieved (>63 µm) surface sample in the BC GeoB20611-1

GeoB206012-1 (Limpopo fan):
Habitat: brown sand, well-sorted, coarse-grained, well oxygenated, subangular to angular grains, quartz, feldspar, rock fragments, and blackish concretions
Fauna: low proportion of biogenic material, low diversity fauna, fragments of bivalves, Echinodermata, Bryozoa, some agglutinated tubes, some Scaphopoda, some snails, some reworked biogenic material, no planktonic foraminiferal species, no ostracods, rare benthic foraminifera (lagenids, *Quinqueloculina*, *Ammonia*)
Interpretation: shallow sublittoral interstitial association

GeoB206013-1 (Limpopo fan):
Habitat: sand with low proportion of detritus, quartz, feldspar or rock fragment very rare, angular grains, small blackish concretions, much glauconite, some faecal pellets
Fauna: fragments of bivalves, Echinodermata, Bryozoa, foraminiferal ooze with dominant planktic foraminifers (globigerinids + *Globorotalia*, *Orbulina*), *Cibicidoides*, and rare lagenids, *Quinqueloculina*, *Textularia*, *Bulimina*, *Uvigerina*, some ostracods, Scaphopoda, rare Polychaeta and some sponge spicules, worm tubes
Interpretation: bathyal globigerinid ooze

GeoB206015-1 (Limpopo fan):
Habitat: brown mud, low proportion of detritus, only few very small quartz grains (angular), high proportion of organic material, colony of tube dwellers
Fauna: many fragments and suspended organic material, fragments of bivalves, Echinodermata, Bryozoa, Pteropoda -fragments, benthic Gastropoda, *Cibicidoides*, globigerinids + *Globorotalia*, *Orbulina*, *Quinqueloculina*, lagenids, Amphipoda, Scaphopoda, some Ostracoda
Interpretation: deep sublittoral soft bottom association

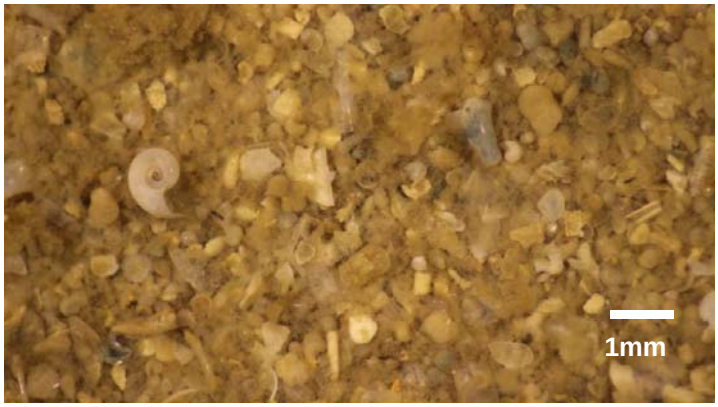

Fig. 4.26 Sieved (>63 µm) surface sample of BC GeoB206015-1

Fig. 4.27 Large, agglutinated foraminifera from BC GeoB206015-1, the test of *Ammodiscus* (lower left) has a diameter of about 1.5 mm

GeoB 206019-1 (off Tugela River):

Habitat: brown mud, very high proportion of detritus, well sorted, fine-grained, angular to subangular quartz and feldspar, lots of mica (greenish), pyrite, rock fragments, small blackish concretions, many faecal pellets and biogenic material

Fauna: some fragments of bivalves, Echinodermata, Bryozoa, snails (some living), Scaphopoda and Bivalvia (some living), rare benthic foraminifera (miliolids, *Ammonia*, lagenids, *Elphidium*), rare planktonic foraminifera (globigerinids, *Orbulina*), very rare Ostracoda, some body parts of Crustacea

Interpretation: sublittoral oxygen poor soft bottom assemblage, shell dissolution

GeoB 20622-1 (off Tugela River)
Habitat: shell detritus with very low proportion of detritus
Fauna: mostly fragments of bivalves, Echinodermata, Bryozoa, rare benthic foraminifera, rare planktonic foraminifera (globigerinids), rare Ostracoda
Interpretation: biogenic intertidal or shallow sublittoral sand (old?)

Fig. 4.28 Sieved (>63 µm) surface sample of BC GeoB206022-1

GeoB 20624-2 (off Mzimvubu River):
Habitat: brown mud, low proportion of detritus, small quartz and feldspar grains (angular), fine-grained, many faecal pellets and high proportion of organic material
Fauna: rare fragments of bivalves, many agglutinated benthic foraminifera (*Rhabdammina abyssorum*, *Bathysiphon*, *Cyclammina*), rare benthic foraminifera (*Pyrgo*), an abundance of planktonic foraminifera (globigerinids, keeled and unkeeled *Globorotalias*, *Orbulina*), rare Pteropoda
Interpretation: bathyal foraminiferal mud

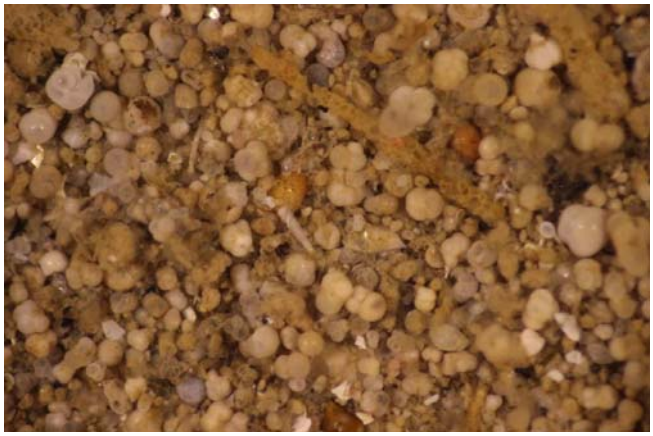

Fig. 4.29 Sieved (>63 µm) surface sample of BC GeoB206024-2

4.5.3 Microfauna From Surface Samples

As expected, the abundance of ostracods was lower than that of foraminiferal assemblages (Fig. 4.30, Tab. 4.2). Ostracods are about ten times less abundant than foraminiferal assemblages and are predominantly missing from high-energy deposits. They show their maximum abundance on the shelf not on the slope as that of foraminifera. In general, the number of both groups is sufficient for quantitative analysis in most samples relying on a few grams of sediment. Living benthic foraminifera were found in almost all samples but in very low proportions only. However, with the exception of two samples containing high proportions of living individuals. The one sample was predominantly mud with calcareous shells bearing dissolution marks and the other was well-sorted sand. Both indicate dissolution and the transport of empty tests explaining the high proportions of living individuals.

Plotting P/B ratios along the water depth gradient indicates a clear correlation and a value of about 50 % for the shelf break as known from literature. Two samples from the slope of the Limpopo area, however, show markedly increased values (Fig. 4.31). Those typical high P/B ratios lie in the centre of the investigated area off the Limpopo mouth. Because benthic foraminiferal numbers are low in this part, increased P/B ratios indicate a higher absolute

number of planktonic foraminiferal assemblages. Higher sedimentation rates of pelagic forms may be explained by inflow and sedimentation within a gyre slowing down in this area.

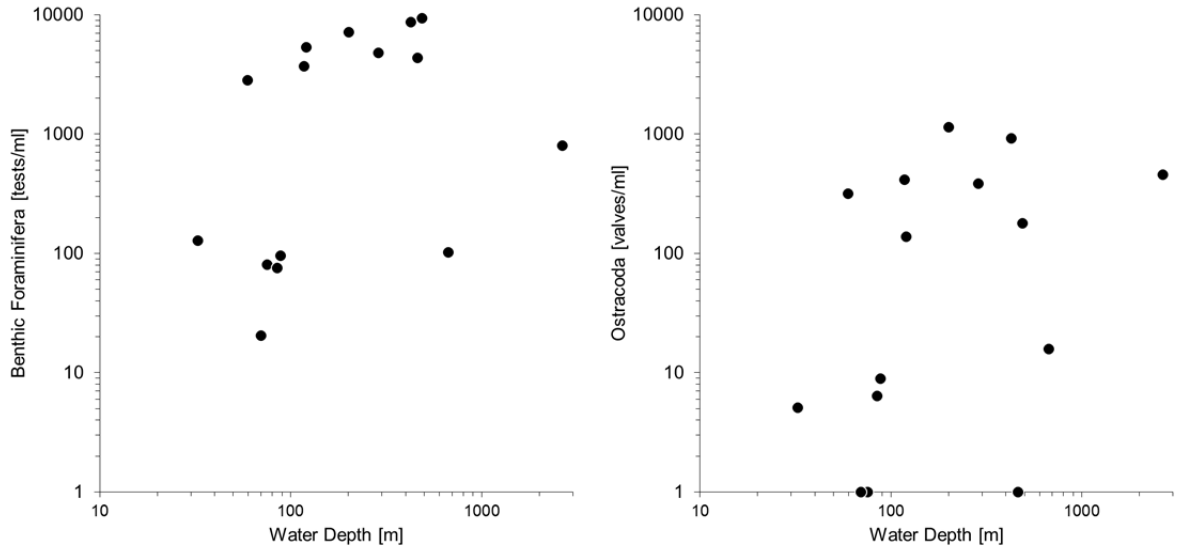

Fig. 4.30 Total abundances (living + dead) of benthic Foraminifera and Ostracoda in surface samples

Table 4.2 Abundance data and water depth for surface samples. The estimated water depth is calculated relying on P/B ratios (excluding sample GeoB20624-2).

Sample	Sediment	water depth [m]	estimated water depth [m]	Ostracoda [valves/ml]	planktic Foraminifera [tests/ml]	benthic Foraminifera [tests/ml]	living benthic Foraminifera [%]	P/B ratio [%]	reworked microfossils [specimens/ml]
GeoB20602-1	sandy mud	117	102	415	2258	3732	3.7	37.7	1336
GeoB20603-1	shell detritus	75	35	1	12	81	0.0	12.5	159
GeoB20604-1	mud	668	386	16	228	102	4.2	69.0	0
GeoB20605-1	coarse sand	69	65	1	8	20	31.3	27.3	41
GeoB20607-1	globigerina ooze	485	375	180	20160	9360	0.0	68.3	0
GeoB20608-2	muddy fine sand	286	813	386	30879	4825	0.0	86.5	0
GeoB20609-1	muddy sand	461	287	1	7141	4375	1.5	62.0	64
GeoB20610-1	fine sandy mud	59	119	317	2016	2851	2.0	41.4	0
GeoB20611-1	fine sandy mud	120	127	138	4055	5391	6.0	42.9	0
GeoB20612-1	coarse sand	88	38	9	17	96	11.3	14.7	101
GeoB20613-1	globigerina ooze	424	1001	922	92621	8755	0.0	91.4	0
GeoB20615-1	organic mud	200	213	1152	8832	7219	3.2	55.0	77
GeoB20619-1	organic mud, angular quartz, rock fragments	32	37	5	20	128	60.0	13.8	3
GeoB20622-1	shell detritus	84	108	6	49	76	3.4	39.2	191
GeoB20624-2	mud	2641	1162	461	14861	806	0.0	94.9	0

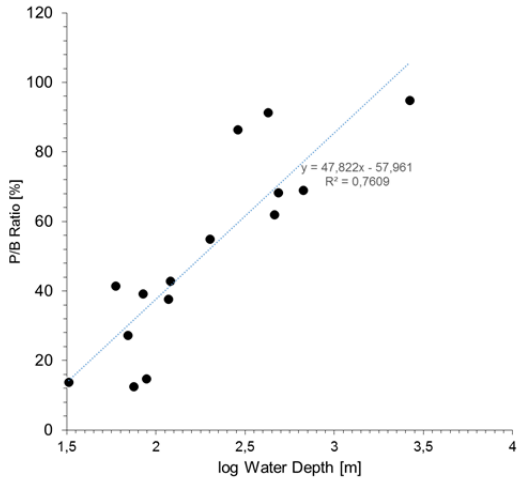

Fig. 4.31 Plankton/Benthos (P/B) ratio of the studied surface samples plotted on water depth

4.5.4 Core GeoB20601-4 From the Western Continental Margin

Facies: Deep marine, olive-gray mud. Non-biogenic grains include glauconite and small angular quartz.

Fauna: Ostracoda (few), Radiolaria (rare), echinoid spines (common), sponge spicules (common), abundant foraminifera (>95% in all sand fraction samples) – planktonic foraminifera more abundant than benthic foraminifera. Planktonic foraminifera include *Globorotalia inflata* (abundant), *Globigerina bulloides* (common), *Orbulina universa* (common), *Globorotalia truncatulinoides* (common), *Globigerinella siphonifera* (few), *Globorotalia hirsuta* (few), *Globorotalia menardii* (few), *Globorotalia* scitula, (occur in some samples), *Globigerinoides ruber* white (few in most samples), *Globigerinoides ruber* pink (rare), *Globigerinoides sacculifer* (rare), *Neogloboquadrina pachyderma* (occur in most samples), *Neogloboquadrina incompta* (occur in some samples), *Neogloboquadrina dutertrei* (occur in most samples), *Orbulina bilobata* (few).

Benthic foraminifera include *Ammonia beccarii* (rare), *Amphicoryna scalaris* (rare), *Brizalina* spp. (common), *Bulimina* spp. (common), *Cassidulina laevigata* (common), *Cibicidoides* spp. (common), *Dentalina* spp. (few), *Eggerella bradyi* (rare), *Ehrenbergina* spp. (rare), *Elphidium advenum* (rare), *Epistominella exigua* (common), *Favulina hexagona* (few in some samples), *Fissurina* spp. (rare), *Fursenkoina bradyi* (few), *Globobulimina* spp. (common), *Gyroidina* sp. (few), *Karreriella bradyi* (rare), *Lagena* spp. (few in most samples), *Lenticulina* spp. (rare), *Lobatula lobatula* (rare), *Martinottiella communis* (rare), *Melonis barleeanum* (few), Miliolids (frequent occurrence), *Nodogenerina* sp. (rare), *Nodosaria* spp. (few), *Nonionella* sp. (few), *Oridorsalis umbonatus* (few), *Plectofrondicularia* sp. (few), *Pullenia bulloides* (few), *Pyrgo* spp. (few), *Sigmoilina* sp. (few), *Siphotextularia* sp. (rare), *Trifarina* sp. (rare), *Uvigerina* spp. (abundant).

Remarks: Many benthic foraminifera indicate a deep marine environment. The abundance of planktonic over benthic foraminifera indicates a depositional environment on the continental slope. The presence of *Ammonia beccarii, Elphidium advenum* and *Lobatula lobatula* among deep-water taxa in the uppermost portion of the core suggests transport from the shelf.

The presence of *Globorotalia truncatulinoides* throughout the core gives the age as Pleistocene.

4.5.5 Cores from the Eastern Continental Margin

Core samples from the eastern continental margin usually have a similar planktonic foraminiferal faunal composition. Abundances of species between cores may vary. Below is a summary of planktonic foraminiferal species and general abundances.

Globigerina bulloides	Only in some cores – low abundance
Globigerinella siphonifera	Occurrence in most cores – generally low abundance
Globigerinoides conglobatus	Common, but generally in low abundances
Globigerinoides ruber	Common (pink forms only in a few cores in very low abundances)
Globigerinoides sacculifer	Common, but generally in very low abundances
Globigerinoides trilobus	Occurrence in most cores in low abundances
Globorotalia inflata	Occurrence in most cores – generally low abundance
Globorotalia menardii	Common
Globorotalia truncatulinoides	Common, but generally in low abundances
Globoturborotalida rubescens pink	Only in a few cores – low abundance
Neogloboquadrina dutertrei	Occurrence in most cores – generally low abundance
Neogloboquadrina pachyderma	Only in some cores – low abundance
Neogloboquadrina incompta	Few
Orbulina bilobata	Few
Orbulina universa	Common
Pulleniatina obliquiloculata	Occurrence in most cores – generally low abundance
Sphaeroidinella dehiscens	Only in a few cores – low abundance

The occurrence and abundance of the warmer water species *Globorotalia menardii* are generally higher in the eastern margin cores as compared to samples from GeoB20601-4 from the western margin; while the dominant planktonic in the core from the western margin *Globorotalia inflata* deceases along the eastern margin. The occurrence and abundance of other warmer water species *Globigerinoides ruber* and *Gs. sacculifer* also increase, although marginally in samples from the eastern margin.

Benthic foraminifera in cores from the eastern margin also reflect warmer water conditions with larger forms present such as *Amphistegina lesonii, Heterostegina depressa* and *Operculina complanata* (Tab. 4.3), and the increase in occurrence and abundance of miliolids (Fig. 4.32).

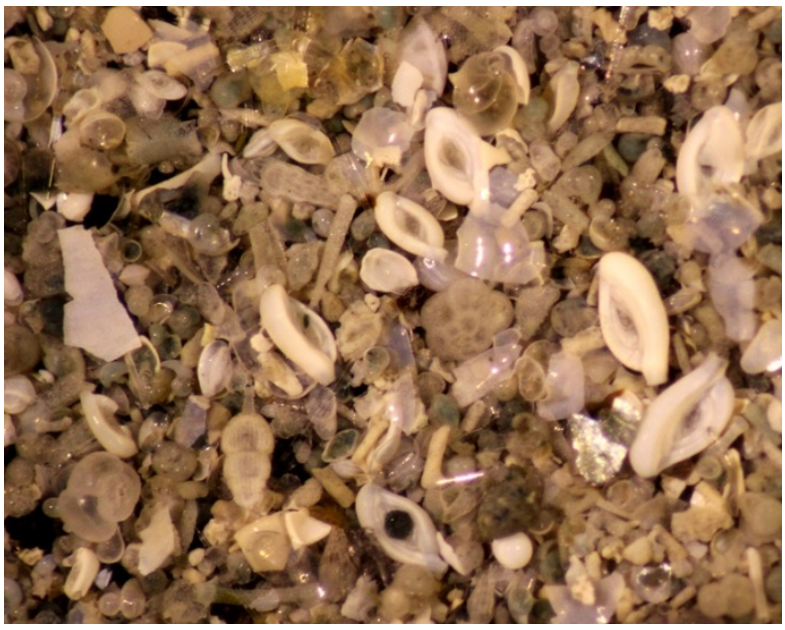

Fig. 4.32
High abundance of *Spiroloculina communis* in core GeoB20615-2

Table 4.3 Benthic foraminifer taxa in gravity cores. Each gravity core is indicated by its number, e.g. GeoB20607-2 is given as 07-2.

	07-2	08-1	09-2	10-2	13-2	15-2	16-1	17-1	20-4	21-1	23-1	24-1
Agglutinids	x	x	x	x	x	x	x	x	x		x	x
Ammonia becarii	x	x		x	x	x	x	x		x	x	x
Amphicoryna spp.	x	x	x	x	x	x	x	x				x
Amphistegina lesonii				x		x						
Anomalinoides sp.			x	x	x	x						
Bolivina sp.							x					x
Brizalina spp.	x	x		x	x	x	x	x			x	x
Bulimina spp.	x	x			x	x	x	x			x	x
Cancris spp.	x		x	x		x	x					x
Cassidulina laevigata	x		x								x	
Chilostomella oolina	x		x			x					x	
Cibicidoides spp.	x	x	x	x	x	x	x	x			x	x
Elphidium spp.				x		x					x	
Fissurina sp.	x	x	x					x				
Frondicularia sp.		x										
Globobulimina sp.	x		x	x		x	x	x			x	x
Globocassidulina subglobosa	x		x		x		x				x	x
Heterostegina depressa	x											
Hyalinea balthica							x	x				x
Lagena sp.	x							x				x
Lenticulina spp.	x	x	x		x	x	x	x			x	x
Lobatula lobatula	x					x	x	x			x	x
Melonis spp.						x	x	x			x	x
Nodosaria spp.	x				x	x	x	x			x	x
Nonion boueanus				x		x						
Nonionella sp.										x		
Operculina complanata				x		x						
Oridorsalis umbonatus	x						x	x				x
Pigmaeaseiston sp.							x					x
Planularia sp.								x				
Pseudorotalia schroeteriana						x						
Pullenia bulloides	x	x	x		x			x				
Pyrgo sp.	x	x	x	x	x	x	x	x	x		x	x
Sigmopyrgo vespertilio	x		x									
Spiroloculina spp.			x	x		x	x	x			x	x
Quinqueloculina sp.	x	x	x	x	x	x	x	x			x	x
Saracenaria italic		x			x							
Siphonina tubulosa					x			x				
Uvigerina (hispid)	x		x		x	x	x	x	x			x
Uvigerina spp. (ribbed)	x	x	x	x	x	x	x	x				x
Vaginulopsis sp.		x				x						

All core catcher samples and additional down core samples, in average ten samples per core, were analysed stratigraphically based on occurrences of planktonic and benthic foraminiferal index species (Tab. 4.4).

Selected samples from cores in the Limpopo fan were analysed for foraminiferal abundances. Qualitative faunal changes within the cores were documented and interpreted preliminary (Fig. 4.33).

Table 4.4 Biostratigraphically constrained maximum ages of sediment cores

GeoB20601-4	max. Plio-Pleistocene
GeoB20607-2	max. Pleistocene
GeoB20608-1	max. Plio-Pleistocene
GeoB20609-2	max. Pleistocene
GeoB20610-2	Holocene
GeoB20613-2	max. Pleistocene
GeoB20615-2	max. Plio-Pleistocene
GeoB20616-1	max. Pleistocene
GeoB20617-1	>MIS38(?)
GeoB20620-4	max. Pleistocene
GeoB20622-2	max. Pleistocene
GeoB20624-1	max. Pleistocene
GeoB20628-1	Upper Cretaceous
GeoB20629-1	Holocene

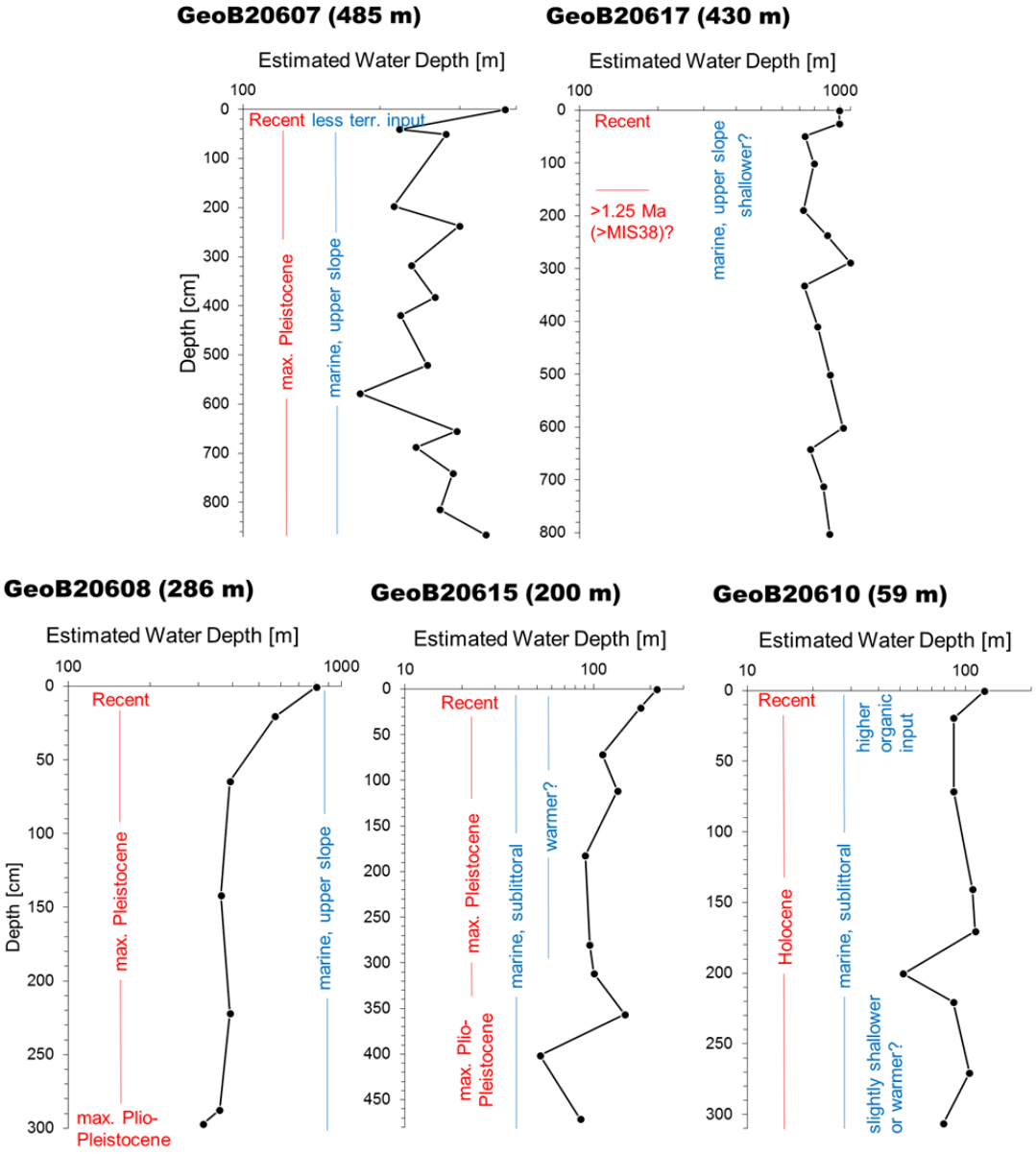

Fig. 4.33 Sediment cores from the Limpopo fan with biostratigraphical information, P/B ratios and preliminary palaeoecological interpretation

4.5.6 Macrofossils for Dating

During description and sampling of the cores, macrofossils were taken for later ^{14}C-dating. Such macrofossils were identified and classified according to their mode of life (Tab. 4.5).

Table 4.5 Macrofossils from sediment cores isolated for ^{14}C dating

core	depth [cm]	Taxon	Preservation	Remarks
GeoB20607-2	184	Gastropoda	well preserved fragment	No
GeoB20607-2	190	*Cavolinia tridentata*	complete, broken	planktic gastropod
GeoB20607-2	190	*Xenophora* sp.	complete, broken	large epibenthic gastropod
GeoB20607-2	417	fragments of benthic and planktic gastropods + bivalves	shell accumulation	allochthonous?
GeoB20607-2	473	*Dentalium* sp.	Complete	shallow endobenthic scaphopod
GeoB20607-2	482	*Limopsis aurita*	one complete valve	epibenthic bivalve
GeoB20607-2	520	*?Tellina* sp.	double valved (autochthonous!)	endobenthic bivalve
GeoB20607-2	541	?*Ctena* sp.	one complete valve	shallow(?) endobenthic bivalve
GeoB20607-2	606	Bryozoa	Fragment	allochthonous?
GeoB20607-2	682	*Cavolinia ?tridentata*	Complete	planktic gastropod
GeoB20607-2	742	*Cuvierina* sp., *?Turritella* sp., *Nuculana* sp.	all complete, but in shell layer	planktic and benthic gastropod + shallow endobenthic bivalve
GeoB20607-2	745	*?Turritella* sp.	Damaged	Gastropod
GeoB20608-1	37	*Cavolinia tridentata*	Complete	planktic gastropod
GeoB20608-1	41	serpulid(?) tube	well preserved fragment	epibenthic, fixosessile
GeoB20608-1	91	*Terebra* sp.	Complete	epibenthic? Gastropod
GeoB20608-1	163	*Marginella* sp.	Complete	Gastropod
GeoB20608-1	CC	*Conus* sp.	almost complete	epibenthic gastropod
GeoB20609-1	MUC	agglutinated tube (Polychaeta or Crustacea)	Fragment	endobenthic filter feeder
GeoB20609-2	31.5	*Cavolinia tridentata*	Complete	planktic gastropod
GeoB20609-2	90	*Cavolinia tridentata*	complete, broken	planktic gastropod
GeoB20609-2	299	*Nuculana* sp.	double valved (autochthonous!)	shallow endobenthic bivalve
GeoB20609-2	316	*?Tellina* sp.	one damaged valve	endobenthic bivalve
GeoB20609-2	398	?*Tellina* sp.	one fragmented valve	endobenthic bivalve
GeoB20609-2	400	Muricidae	complete, damaged, with balanids	epibenthic? Gastropod
GeoB20609-2	413	*Cavolinia tridentata*	Complete	planktic gastropod
GeoB20609-2	367-467	*Cuvierina* sp.	Complete	planktic gastropod
GeoB20609-3	604	*?Turritella* sp.	slightly damaged	Gastropod
GeoB20610-2	15	*Cerastoderma* sp. + gastropod fragment	one large fragment each	shallow endobenthic bivalve
GeoB20610-2	52	*Cerastoderma* sp.	one complete valve	shallow endobenthic bivalve
GeoB20610-2	69	*Macoma* sp.	one complete valve	shallow endobenthic bivalve
GeoB20610-2	71	*Macoma* sp.	one complete valve	shallow endobenthic bivalve
GeoB20610-2	86	*Macoma* sp.	double valved (autochthonous!)	shallow endobenthic bivalve
GeoB20610-2	95	*Limopsis aurita*	one complete valve	epibenthic bivalve
GeoB20610-2	127	*?Muricopsis* sp.	Complete	Gastropod
GeoB20610-2	271	*Pisanianura ?grimaldii*	Complete	Gastropod
GeoB20610-2	292	*Terebra* sp.	one slightly damaged shell	epibenthic? Gastropod
GeoB20613-2	215.5	Scleractinia	fragmented (complete?)	solitary coral
GeoB20613-2	241	*?Nasopharus* sp.	one valve, fragmented	deep endobenthic bivalve
GeoB20615-2	277	*Cerithium* sp.	Complete	epibenthic gastropod
GeoB20615-2	355	Wood	Fragment	terrestrial
GeoB20616-1	632	*Limopsis aurita*	double valved (autochthonous!)	epibenthic bivalve
GeoB20616-1	634	*?Turritella* sp.	slightly damaged	gastropod
GeoB20616-1	664	Scleractinia	Complete	solitary coral
GeoB20617-1	195	*?Xenophora* sp.	crushed fragment	epibenthic gastropod
GeoB20621-1	695	?*Tellina* sp. + attached balanids	complete valve	endobenthic bivalve
GeoB20628-1	54	*Turritella* sp.	slightly damaged	gastropod
GeoB20628-1	187.5	*Mactra* sp.	complete valve	infaunal bivalve

4.6 Plankton Sampling

(Siccha, M., Strachan, K, Hoffmann, D., Kossack, M.)

4.6.1 Sampling and Sample Preparation

The purpose of plankton sampling was the collection of planktic foraminifera for molecular genetic studies and habitat characterization. Sampling was conducted with a Multi Plankton Sampler (MPS) [HydroBios, Kiel, Germany]. The used device has a 50 × 50 cm opening and five net bags with 100 µm mesh diameter. A water sampler with 5 niskin bottles (1.8 L volume) and a CTD M90 [Sea and Sun Technology, Trappenkamp, Germany] were mounted on the body of the MPS.

A total of 6 stations were sampled with 19 individual MPS casts. Three standard sampling depth schemes with fixed sampling interval boundaries were used at each station; a deep cast with a maximum depth of 700 m (700–500–300–200–100–0 m sampling interval boundaries), a shallow cast with a maximum depth of 100 m (100–80–60–40–20–0 m sampling interval boundaries), and a filter cast with a maximum depth of 500 m (500–300–150–80–40–0 m sampling interval boundaries). Exceptions to this pattern were stations GeoB20626, where the filter cast sampling scheme was used twice in succession. Closing depths for all strict vertical net hauls were based on depth calculated from pressure readings of the pressure sensor on the net body. Slacking and hoisting was done at 0.5 m/s rope speed. The water sampler was used to obtain water samples for δ13C and δ18O analysis. The attached CTD recorded temperature, salinity, oxygen, chlorophyll *a* and pH in one decibar intervals for the MPS deployments. The net bags of the MPS were washed with sea water and inspected for damage after each net haul; the net cups were rinsed and cleaned with filtered sea between deployments and in an ultrasonic bath between stations.

The samples obtained from the first (deep) and second (shallow) MPS cast were mostly conserved as plankton concentrates, a few samples were picked that is the planktic foraminifera extracted under stereo-microscopes and transferred onto micropaleontological sample slides. Plankton concentrates and sample slides were deep frozen at .80°C. The samples of the third (filter) MPS cast at each station were dedicated to the genetic analysis via Next-Generation-Sequencing (NGS). The obtained plankton concentrates from this net haul were filtered over 8-12 µm pore size cellulose filters in a vacuum filtration system. Samples were wet-sieved over 1000 µm sieves to remove the larger zooplankton organisms before filtration. The canisters and filter caskets were carefully cleaned between filtration of different samples to avoid contamination. The obtained filters were deep frozen and stored at -80°C. All frozen samples, slides, plankton concentrates and filters will be shipped with dry ice to the University of Bremen at the end of cruise M126. Water for isotope analysis was obtained from the deep and shallow casts in 2 ml (δ18O) and 15 ml (δ13C) vials. Water samples for δ13C analysis were poisoned with 45 µl saturated Mercury chloride solution.

The sampling conditions for the MPS were difficult due to the strong current of up to 6 knots at several sites within the Agulhas. The angle of the ship's rope to the MPS in the water reached values of 45° resulting in a quasi semi-horizontal tow. The attached water sampler suffered from mechanical malfunction at the beginning of the cruise so that water could not be sampled during all casts. The CTD suffered from problems with its power supply, so that casts could only be recorded at three of the six sites of deployment.

4.6.2 Plankton Sampling Preliminary Results

Without the detailed counting results, preliminary results are limited. Since we want to conserve all samples for an eventual genetic analysis, we aimed at freezing the samples as soon as possible. So only a few samples were visually inspected and the planktic foraminifera extracted. The foraminifera assemblage was very diverse as was expected for this region. Among the identified species were: *Hastigerina pelagica*, *Globigerinella siphonifera*, *Sphaeroidinella dehiscens*, *Trilobatus sacculifer*, *Globigerinoides ruber*, *Globigerinoides conglobatus*, *Globoturborotalita rubescens*, *Turborotalita humilis*, *Neogloboquadrina dutertrei*, *Globorotalia truncatulinoides*, *Globorotalia menardii* and *Globorotalia scitula*.

The available co-registered CTD data show that we sampled three different water masses: the mixed surface layer, the *Subtropical Mode Water* (STMW) and the upper part of the *Antarctic Intermediate Water* (AAIW) (Fig. 4.34). Maximal chlorophyll concentrations of up to 2 µg/L were found in a thin a deep chlorophyll maximum below the pycnocline at depths between 60 and 115 m.

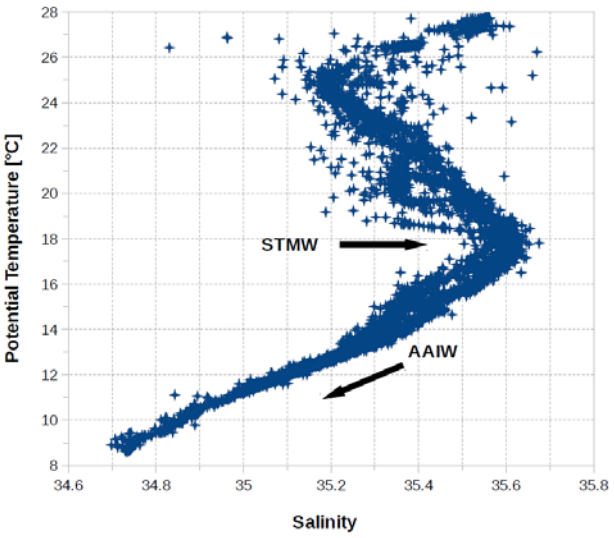

Fig. 4.34
TS-diagram of waters sampled with the MPS. (all available CTD data merged)

Table 4.6 Multi Plankton Sampler sampling stations during cruise M123

Station GeoB206#	Date	Latitude	Longitude	Plankton samples	CTD	Water samples
01-1	5.2.2016	31° 59,78' S	15° 58,18' E	5	-	-
01-2	5.2.2016	31° 59,78' S	15° 58,18' E	5	-	-
01-3	5.2.2016	31° 59,78' S	15° 58,18' E	2	-	-
06-1	11.2.2016	27° 54,71' S	32° 58,20' E	5	X	10
06-2	11.2.2016	27° 54,86' S	32° 58,04' E	5	X	10
06-3	11.2.2016	27° 54,89' S	32° 58,02' E	5	X	-
18-1	17.2.2016	29° 02,07' S	32° 26,74' E	5	-	-
18-2	17.2.2016	29° 03,37' S	32° 26,03' E	5	X	10
18-3	17.2.2016	29° 03,83' S	32° 25,75' E	5	X	6
20-1	18.2.2016	31° 10,36' S	32° 08,88' E	5	X	10
20-2	18.2.2016	31° 10,36' S	32° 08,88' E	5	X	10
20-3	18.2.2016	31° 10,36' S	32° 08,88' E	5	X	-

Table 4.6 Multi Plankton Sampler sampling stations during cruise M123 (*continuation*)

Station GeoB206#	Date	Latitude	Longitude	Plankton samples	CTD	Water samples
26-1	22.2.2016	33° 06,48' S	28° 21,60' E	5	-	8
26-2	22.2.2016	33° 08,36' S	28° 18,87' E	5	-	10
26-3	22.2.2016	33° 08,78' S	28° 18,12' E	5	-	-
26-4	22.2.2016	33° 10,06' S	28° 16,63' E	5	-	-
27-1	23.2.2016	34° 26,44' S	26° 14,98' E	5	-	-
27-2	23.2.2016	34° 28,17' S	26° 12,19' E	5	-	10
27-3	23.2.2016	34° 28,66' S	26° 11,31' E	4	-	4

4.7 Sampling of Surface Water Suspended Material

(E. Schefuß)

To analyse the distributions of algal lipids and their isotopic signatures, surface water suspended particulate organic matter was sampled using the vessel's rotary pump. The water was filtered through pre-combusted glass fibre filters (GF/F, Whatman). After sampling, the filters were wrapped in pre-combusted aluminium foil and dried at 40°C for several days. To determine the isotopic fractionation between the surface water and lipids, two 2-ml water samples were taken at each sampling transect, one at the beginning and one at the end. The water samples were not poisoned. The water bottles were thoroughly closed with lids and stored at room temperature. The water samples are numbered according to the filter samples, #-I for the sample taken at the start of a sample transect and #-II for the sample taken at its end.

Table 4.7 List of suspended particulate organic matter samples. Sea-surface temperature (SST) and salinity (SSS) are derived from the ship's thermosalinograph.

No.		Date	Time	Latitude			Longitude			SST	SSS	Volume
			(UTC)	deg	min		deg	min		°C	Psu	Liters
1	Start	04.02.16	12:25	27	15.637	S	14	49.327	E	16.440	34.92	69
	Stop		12:58		21.085			50.665		16.670	34.92	
2	Start	04.02.16	17:13	28	1.178	S	15	0.615	E	20.760	34.82	169
	Stop		17:58		7.738			2.229		20.890	34.84	
3	Start	05.02.16	6:52	30	13.215	S	15	33.853	E	20.080	34.85	134
	Stop		8:25		29.322			37.959		20.490	34.98	
4	Start	05.02.16	13:52	31	23.708	S	15	51.908	E	20.800	35.17	152
	Stop		15:22		38.780			55.796		19.570	35.15	
5	Start	06.02.16	10:42	33	29.583	S	17	10.966	E	21.040	35.28	288
	Stop		12:48		45.730			25.668		18.910	35.13	
6	Start	06.02.16	17:16	34	17.917	S	17	55.701	E	21.970	35.33	256
	Stop		18:42		26.841		18	7.353		22.300	35.32	
7	Start	07.02.16	8:31	35	14.689	S	20	14.587	E	22.890	35.43	438
	Stop		10:27		12.525			38.351		22.040	35.29	
8	Start	07.02.16	17:38	35	5.813	S	22	7.760	E	19.300	34.86	120
	Stop		18:12		4.960			14.660		19.030	34.86	
9	Start	08.02.16	7:30	34	28.180	S	24	44.807	E	18.790	35.15	130
	Stop		9:13		23.478			16.912		18.780	35.06	
10	Start	08.02.16	17:12	33	57.482	S	26	34.079	E	19.960	35.25	168
	Stop		10:00		54.579			42.581		21.380	35.30	

Table 4.7.1 List of suspended particulate organic matter samples. Sea-surface temperature (SST) and salinity (SSS) are derived from the ship's thermosalinograph. (*continuation*)

No.		Date	Time	Latitude			Longitude			SST	SSS	Volume
			(UTC)	deg	min		deg	min		°C	Psu	Liters
11	Start	09.02.16	7:32	32	50.922	S	28	20.201	E	24.940	35.24	367
	Stop		9:35		42.983			39.139		25.650	35.25	
12	Start	09.02.16	16:48	31	52.638	S	29	31.244	E	26.510	35.33	285
	Stop		17:27		46.877			34.327		26.240	35.32	
13	Start	10.02.16	12:28	29	54.923	S	31	25.411	E	27.700	35.28	441
	Stop		13:44		41.177			32.948		27.170	35.27	
14	Start	10.02.16	16:58	29	13.887	S	31	42.518	E	25.460	35.23	220
	Stop		17:44		12.942			42.506		25.430	35.22	
15	Start	11.02.16	9:59	27	54.166	S	33	0.530	E	27.340	35.27	726
	Stop		12:56		35.006			26.552		28.080	35.29	
16	Start	11.02.16	16:25	27	3.849	S	33	50.143	E	27.800	35.22	518
	Stop		17:38	26	52.802			58.476		27.810	35.26	
17	Start	12.02.16	11:28	25	28.814	S	35	15.065	E	27.270	35.28	466
	Stop		12:37		27.875			20.291		27.420	35.38	
18	Start	13.02.16	9:21	25	36.184	S	33	51.699	E	27.730	35.34	584
	Stop		11:10		25.514			48.740		27.410	35.34	
19	Start	14.02.16	12:12	25	10.997	S	34	9.475	E	27.440	35.31	553
	Stop		13:59		12.873		33	47.500		27.650	35.36	
20	Start	15.02.16	12:52	25	35.411	S	33	20.114	E	27.530	35.26	542
	Stop		14:33		26.512			30.216		27.880	35.38	
21	Start	16.02.16	10:52	26	6.724	S	33	40.752	E	27.290	35.32	488
	Stop		12:18		21.672			35.306		27.000	35.36	
22	Start	17.02.16	11:08	29	29.385	S	31	44.867	E	22.990	35.26	278
	Stop		12:17		24.601			40.772		23.260	35.21	
23	Start	17.02.16	14:48	29	13.628	S	31	34.102	E	24.700	35.24	92
	Stop		15:48		10.861			39.642		24.690	35.25	
24	Start	18.02.16	9:31	31	10.713	S	32	8.010	E	26.470	35.15	704
	Stop		11:23		10.360			8.907		26.480	35.16	
25	Start	19.02.16	12:20	30	2.846	S	31	15.614	E	24.050	35.20	293
	Stop		13:27		14.529			3.678		24.720	35.20	
26	Start	20.02.16	11:10	31	44.382	S	29	41.110	E	24.940	35.23	472
	Stop		12:40		39.355			48.169		24.140	35.21	
27	Start	21.02.16	13:58	31	52.034	S	29	52.263	E	24.980	35.26	298
	Stop		15:03		52.032			52.263		25.050	35.26	
28	Start	22.02.16	13:48	32	53.981	S	28	14.719	E	24.280	35.22	333
	Stop		15:00	33	4.880			20.584		25.580	35.22	
29	Start	23.02.16	9:20	34	22.919	S	25	25.253	E	20.970	35.18	171
	Stop		10:04		21.196			15.178		21.120	35.20	
30	Start	24.02.16	10:21	34	33.996	S	21	5.482	E	21.730	35.09	217
	Stop		11:15		39.885		20	58.078		21.550	35.08	

(Base on the continuously sampling, these samples got neither a station number nor a GeoB number)

4.8 Water Sampling

(M. Humphries, K. Strachan)

Surface water samples for radium isotope analysis (^{226}Ra and ^{228}Ra) were collected at 15 sites along the South African coast (Tab. 4.8). Sampling focused specifically on the western and southern margins of the country in order to compliment data already obtained from the east

coast. Samples were recovered using the vessel's seawater line and therefore did not require any station time. At each sampling station, 210 L of seawater was collected and then pumped through an acrylic MnO_2 fibre at a flow rate of <1 L min^{-1}. Fibre samples were then bagged and stored for analysis.

Table 4.8 Radium isotope water sampling locations

Sample ID	Date of collection	Time filtering stopped	Latitude	Longitude	Remark
M123-1	05/02/2016	15:20	30° 11.9 S	15° 33.5 E	West coast
M123-2	05/02/2016	21:32	31° 20.14 S	15° 50.98 E	West coast
M123-3	06/02/2016	09:20	32° 06.70 S	15° 52.10 E	West coast
M123-4	06/02/2016	14:10	33° 08.25 S	16° 51.58 E	West coast, Saldanha Bay
M123-5	06/02/2016	22:10	34° 06.99 S	17° 45.08 E	West coast, Cape Town
M123-6	13/02/2016	13:30	24° 54.30 S	34° 48.38 E	Maputo Bay
M123-7	14/02/2016	07:00	25° 11.405 S	33° 45.27 E	Maputo Bay
M123-8	15/02/2016	14:15	25° 33.85 S	33° 03.998 E	Maputo Bay
M123-9	22/02/2016	19:46	32° 49.53 S	28° 10.11 E	South coast, EL
M123-10	23/02/2016	18:35	34° 18.797 S	25° 01.157 E	South coast, St Francis Bay
M123-11	24/02/2016	06:25	34° 12.886 S	23° 52.578 E	South coast, Plettenberg Bay
M123-12	24/02/2016	10:31	34° 28.871 S	21° 40.722 E	South coast, Still Bay
M123-13	25/02/2016	16:00	34° 05.700 S	22° 36.008 E	South coast, Wilderness
M123-14	26/02/2016	14:10	35° 05.454 S	19° 58.791 E	South coast, Cape Agulhas
M123-15	26/02/2016	21:02	34° 46.681 S	19° 02.699 E	South coast, Danger Point

(Base on the continuously sampling, these samples got neither a station number nor a GeoB number)

5 Ship's Meteorological Station

(C. Rohleder, M. Stelzner)

On the 3th of February about nine o'clock local time R/V METEOR left the harbor of Walvis Bay/Namibia to this expedition. At this time a trough extended over the coast of southwestern Africa from the tropical low-pressure area to south. Between low pressure on the African continent and the slowly reinforcing and shifting southeast anticyclone above the South Atlantic it came on the first night of the journey to strong southerly winds to 6 Beaufort. The significant wave height increased until the morning of the second day to 3,5 m. On Friday, the 5th of February, RV Meteor reached the first working station of this trip. At low pressure influence the weather conditions were ideal with southern wind at Beaufort 4 and a significant wave height of 1.5 to 2 m.

For the onward journey to the Cape of Good Hope a cyclone from the west was forecasted, its front finally reached the Cape in the night to Sunday. In the evening of 6th of February RV Meteor passed the Table Mountain and the Cape of Good Hope in good weather conditions. The storm reached the ship not until the following night. At the same time drew a cyclone drew east of Mozambique to the south. Overall, cool and unstable air flowed in the sailing area, which accompanied the weather until the second week of the expedition. Passing Cape Agulhas, RV Meteor left the Atlantic Ocean and arrived at the Indian Ocean. Some rain showers, significant wave heights from 2 to 3 m and wind speeds in the range of 5–6 Beaufort dominated the next few days of the transit to the first working area.

Around the 9th of February R/V METEOR arrived in the area of the Agulhas Current. This ocean current along the east coast of Africa is transporting huge amounts of warm water to the south. This caused air temperatures above the 25°C mark for the followed days of this leg. R/V METEOR arrived at the first working area on the mouth of the river Limpopo in Mozambique on 12th of February. When the station work began, there were weak winds from south, caused by low pressure opposites. Similar weather conditions prevailed also for the rest of the days until the end of the research on the coast of Mozambique.

On Tuesday, the 16th of February, R/V METEOR left the first working area. A trough of low pressure along the southwest African coast caused weak wind from variable directions on the sail to south. Meantime the working area 2 came under the influence of a wedge of a high, which moved from west over the coast of South Africa. This wedge shifted slowly to south. At the same time a new area of low pressure formed over the south of South Africa. Thereby the air pressure differences were increased. The wind freshened appreciably. The morning of the 18th of February was marked by sometimes heavy rain. The amount of precipitation during this rain period was circa 110 liters/square meter. The station work was nevertheless continued. In the afternoon calmed down the weather.

At 18th of February, it was decided, to repeat a working station about 100 nm to northeast. Therefore, the ship sailed that afternoon in this direction. On this path R/V METEOR crossed a thunderstorm area, which, starting from the said low pressure area, spread out of the coastal area. In the early evening lightning was observed, short time later the ship was in a strong, widely extended thunderstorm cell, which further moved in the late night to the southeast. Strong gusts (highest wind speed 16.7 m/s) and waves prevented the sail of the ship. The working station was reached on the next morning and could be finished with a clear sky and best working conditions after deduction of thunderstorm cell.

On the way back to the primary route, the weather was sunny with northeasterly winds about 4 Beaufort and a swell about 1.5 to 2 m. The low on the South African coast strengthened during the day on its southern side, moved slowly southeastward and caused rain showers and thunderstorms again. During the first use of the vibrocorer in the evening of the 19th of February lightning could be observed in the coastal areas. Unfortunately, technical problems delayed the recovery of the device and a thunderstorm reached the R/V METEOR before the work was completed. With wind about 7 Beaufort, increased waves and moderate rain showers, the problem had to be solved despite strong lightning activity, which ultimately succeeded.

In the further course of the sail a new wedge of a high moved slowly from west into the working area. Later this wedge became a high pressure center in the east of the working area. On 20th of February there was a significant wave high around 4 m, the wind blew with 8 Beaufort and there have been occasional rain showers. On Sunday, 21th of February, the weather conditions calmed noticeably. An eastward shifting polar low pressure zone with several low pressure centers south of the Cape of Good Hope influenced the last working area only on Tuesday, the 23th of February with increasing swell around 3m. On Thursday, 25th of February the last station could be finished in good weather conditions.

In the morning of 26th of February R/V METEOR passed the Cape of Good Hope again. A trail of a cyclone which was passing the southern point of Africa on Friday, caused wind with 7–8 Beaufort and a significant wave high around 3m again.

In the morning of the 27th of February R/V METEOR arrived at Cape Town.

6 Station List M123

(M. Zabel, A. Hahn)

Table 6.1 Station list M123

Station Nr	GeoB Nr	Gear*	Date	Time	Lat (S)	Long (E)	Water Depth (m)	Recovery (cm)
m123_160-1	20601-1	MPS-700	05.02.16	22:45:00	31°59.780'	15°58.180'	874	
m123_160-2	20601-2	MPS-100	05.02.16	22:45:00	31°59.783'	15°58.184'	874	
m123_160-3	20601-3	MPS-500	05.02.16	22:45:00	31°59.783'	15°58.184'	874	
m123_160-4	20601-4	GC-12	05.02.16	22:45:00	31°59.783'	15°58.184'	874	868
m123_161-1	20602-1	BC	08.02.16	16:45:00	34° 2.241'	26°20.301'	117	
m123_162-1	20603-1	BC	09.02.16	06:45:00	32°51.971'	28°15.987'	75	
m123_163-1	20604-1	BC	09.02.16	19:13:00	31°42.310'	29°38.040'	668	
m123_164-1	20605-1	BC	10.02.16	19:46:00	29°11.506'	31°41.452'	69	
m123_165-1	20606-1	MPS-700	11.02.16	08:00:00	27°54.863'	32°58.039'	1227	
m123_165-2	20606-2	MPS-100	11.02.16	08:00:00	27°54.863'	32°58.039'	1227	
m123_165-3	20606-3	MPS-500	11.02.16	08:00:00	27°54.863'	32°58.039'	1227	
m123_166-1	20607-1	MC	12.02.16	02:00:00	25°49.262'	34°46.153'	485	
m123_166-2	20607-2	GC-12	12.02.16	02:00:00	25°49.262'	34°46.153'	485	870
m123_167-1	20608-1	GC-12	12.02.16	06:00:00	25°36.711'	34°43.320'	286	273**
m123_167-2	20608-2	MC	12.02.16	06:00:00	25°36.711'	34°43.320'	286	
m123_168-1	20609-1	MC	12.02.16	14:31:00	25°31.658'	35° 3.590'	461	
m123_168-2	20609-2	GC-12	12.02.16	14:33:00	25°31.658'	35° 3.590'	461	831
m123_169-1	20610-1	BC	14.02.16	08:00:00	25° 2.696'	34°43.543'	59	
m123_169-2	20610-2	GC-6	14.02.16	08:00:00	25° 2.696'	34°43.543'	59	321
m123_170-1	20611-1	BC	14.02.16	08:33:00	25° 8.352'	34°40.300'	120	
m123_170-2	20611-2	GC-6	14.02.16	08:33:00	25° 8.352'	34°40.300'	120	empty
m123_171-1	20612-1	BC	14.02.16	17:30:00	25°14.233'	33°45.880'	88	
m123_172-1	20613-1	BC	14.02.16	18:00:00	25°45.451'	33°54.289'	424	
m123_172-2	20613-2	GC-6	14.02.16	18:00:00	25°45.451'	33°54.289'	424	463
m123_173-1	20614-1	BC	15.02.16	09:10:00	25°32.489'	33°10.135'	51	
m123_174-1	20615-1	BC	15.02.16	11:04:00	25°33.073'	33°12.181'	200	
m123_174-2	20615-2	GC-6	15.02.16	11:04:00	25°33.073'	33°12.181'	200	532
m123_175-1	20616-1	GC-12	15.02.16	13:00:00	25°35.395'	33°20.084'	460	957
m123_176-1	20617-1	GC-12	16.02.16	08:00:00	25°36.442'	33°51.795'	430	862
m123_177-1	20618-1	MPS-700	17.02.16	04:30:00	29°03.330'	32°26.070'	1290	
m123_177-2	20618-2	MPS-100	17.02.16	04:30:00	29°03.330'	32°26.070'	1272	
m123_177-3	20618-3	MPS-500	17.02.16	04:30:00	29°03.330'	32°26.070'	1290	
m123_178-1	20619-1	BC	17.02.16	18:30:00	29°15.965'	31°33.525'	32	
m123_178-2	20619-2	GC-6	17.02.16	18:30:00	29°15.965'	31°33.525'	32	600
m123_178-3	20619-3	GC-12	17.02.16	18:30:00	29°15.965'	31°33.525'	32	826
m123_179-1	20620-1	MPS-700	18.02.16	08:30:00	31°10.459'	32°08.637'	3059	
m123_179-2	20620-2	MPS-100	18.02.16	08:30:00	31°10.459'	32°08.637'	3059	
m123_179-3	20620-3	MPS-500	18.02.16	10:30:00	31°10.459'	32°08.637'	3059	
m123_179-4	20620-4	GC-12	18.02.16	12:30:00	31°10.459'	32°08.637'	3059	387**
m123_179-5	20620-5	BC	18.02.16	13:30:00	31°10.459'	32°08.637'	3059	

Table 6.1 Station list M123 (*continuation*)

Station Nr	GeoB Nr	Gear*	Date	Time	Lat (S)	Long (E)	Water Depth (m)	Recovery (cm)
m123_180-1	20621-1	GC-12	19.02.16	07:24:00	29°15.981'	31°33.490'	34	717
m123_181-1	20622-1	BC	19.02.16	18:40:00	30°45.301'	30°35.520'	85	
m123_181-2	20622-2	VC	19.02.16	18:40:00	30°45.301'	30°35.520'	85	399
m123_182-1	20623-1	GC-6	21.02.16	10:45:00	31°42.294'	29°38.034'	671	316
m123_183-1	20624-1	GC-6	21.02.16	13:32:00	31°52.034'	29°52.273'	2644	600
m123_183-2	20624-2	BC	21.02.16	14:32:00	31°52.034'	29°52.273'	2643	
m123_184-1	20625-1	BC	22.02.16	12:10:00	32°49.530'	28°20.110'	37	
m123_185-1	20626-1	MPS-700	24.02.16	16:00:00	33°06.480'	28°21.060'	1259	
m123_185-2	20626-2	MPS-100	24.02.16	16:00:00	33°06.480'	28°21.060'	1259	
m123_185-3	20626-3	MPS-500	24.02.16	16:00:00	33°06.480'	28°21.060'	1259	
m123_185-4	20626-4	MPS-500	24.02.16	16:00:00	33°06.480'	28°21.060'	1259	
m123_186-1	20627-1	MPS-700	24.02.16	05:32:00	34°29.690'	26°11.310'	1267	
m123_186-2	20627-2	MPS-100	24.02.16	05:32:00	34°29.690'	26°11.310'	1267	
m123_186-3	20627-3	MPS-500	24.02.16	05:32:00	34°29.690'	26°11.310'	1267	
m123_187-1	20628-1	VC	24.02.16	10:30:00	34°33.880'	21°05.670'	71	436
m123_188-1	20629-1	VC	25.02.16	06:43:00	34°05.605'	22°35.993'	50	499

* gear types: BC – box corer, GC – gravity corer, MC – multicorer, MPS – multi plankton sampler, VC – vibrocorer
** bent core barrel ("banana")

7 Data and Sample Storage and Availability

All metadata were delivered to the PANGAEA World Data Center MARE and to the BSH (CSR) immediately after the cruise. The ship station list is published together with the SCR on the homepage of the control station METEOR. Geological cores are stored in the MARUM core repository. These and the other geological samples have obtained GeoB ID numbers in addition to the PANGAEA event labels. All analytical data, which will be gained from cruise samples will also be delivered to the PANGAEA WDC MARE.

Type	*Database*	*Available*	*Free Access*	*Contact*
hydrography		March 2016	March 2016	
raw data / CTD	PANGAEA	March 2016	March 2016	lgerullis@marum.de
analytical data	PANGAEA	As soon as they were gained	July 2018	mzabel@marum.de

8 Acknowledgements

The overall successful course of this expedition needs to be attributed to the friendly cooperation and very efficient technical assistance of Captain Michael Schneider, his officers and crew. No matter in which area, we always were attentively cared for. It was always obvious that all people on board worked on a common task. For this we would like to thank everybody involved, last but not least also the Leitstelle METEOR Hamburg. We would like to cordially thank Götz Ruhland (MARUM/Bremen University), Klaus Bohn (LPL Projects + Logistics GmbH) and their teams for professional support of expedition logistics.

The expedition was funded by the Federal Ministry of Education and Research (BMBF; 03F0731A) and strongly supported by MARUM.

9 References

Andò, S., Garzanti, E., Padoan, M., Limonta, M., 2012. Corrosion of heavy minerals during weathering and diagenesis: A catalog for optical analysis. Sedimentary Geology 280, 165-178.

Birch, G.F., Rogers, J., Bremner, J.M., 1986. Marine Geoscience Map Series: Texture and composition of surficial sediments of the continental margin of the Republics of South Africa, Transkei and Ciskei. 1 pp.

Boyce, R.E., 1968. Electrical resistivity of modern marine sediments from the Bering Sea. J. Geophys. Res. 73, 4759-4766.

Cawthra, H.C., 2014. The marine geology of Mossel Bay. Ph.D. Thesis, University of Cape Town, 283pp.

Cawthra, H.C., Bateman, M. D., Carr, A. S., Compton, J. S., Holmes, P. J., 2014. Understanding Late Quaternary change at the land–ocean interface: a synthesis of the evolution of the Wilderness coastline, South Africa. Quaternary Science Reviews 99, 210-223.

Dingle, R.V., Birch, G.F., Bremner, J.M., De Decker, R.H., Du Plessis, A., Engelbrecht, J.C., Fincham, M.J., Fitton, T., Flemming, B.W., Gentle, R.I., Goodlad, S.W., Martin, A.K., Mills, E.G., Moir, G.J., Parker, R.J., Robson, S.H., Rogers, J., Salmon, D.A., Siesser, W.G., Simpson, E.S.W., Summerhayes, C.P., Westall, F., Winter, A., Woodborne, M.W., 1987. Deep-sea sedimentary environments around southern Africa (south-east Atlantic and south-west Indian oceans. Annals of the South African Museum, 98(1).

Galehouse J.S., 1971. Point counting. In: Carver, R.E. (Ed.) Procedures in sedimentary petrology. Wiley, New York, 385–407.

Garzanti, E., Vermeesch, P., Padoan, M., Resentini, A., Vezzoli, G., Andò, S., 2014. Provenance of Passive-Margin Sand (Southern Africa). The Journal of Geology 122 (1), 17-42.

Green, A.N., Cooper, J.A.G., Salzmann, L., 2014. Geomorphic and stratigraphic signatures of meltwater pulses on continental shelves. Geology 42, 151-154.

Mange, M.A., Maurer, H.F.W., 1992. Heavy minerals in colour. London, Chapman and Hall, pp. 147.